

Online Kernel CUSUM for Change-Point Detection

Song Wei and Yao Xie*

H. Milton Stewart School of Industrial and Systems Engineering
Georgia Institute of Technology, Atlanta, Georgia, 30332, U.S.A.

Abstract

We present a computationally efficient online kernel Cumulative Sum (CUSUM) method for change-point detection that utilizes the maximum over a set of kernel statistics to account for the unknown change-point location. Our approach exhibits increased sensitivity to small changes compared to existing kernel-based change-point detection methods, including Scan-B statistic, corresponding to a non-parametric Shewhart chart-type procedure. We provide accurate analytic approximations for two key performance metrics: the Average Run Length (ARL) and Expected Detection Delay (EDD), which enable us to establish an optimal window length to be on the order of the logarithm of ARL to ensure minimal power loss relative to an oracle procedure with infinite memory. Moreover, we introduce a recursive calculation procedure for detection statistics to ensure constant computational and memory complexity, which is essential for online implementation. Through extensive experiments on both simulated and real data, we demonstrate the competitive performance of our method and validate our theoretical results.

Keywords: Change-point detection; Cumulative Sum; Kernel method; Maximum Mean Discrepancy; Online algorithm.

*Author correspondence to Yao Xie (e-mail: yao.xie@isye.gatech.edu).

1 Introduction

Online change-point detection is a fundamental and classic problem in statistics and related fields. The goal is to detect a change in the underlying data distribution as quickly as possible after the change has occurred while maintaining a false alarm constraint. Traditional approaches are based on parametric models that detect changes in distribution parameters, such as the Shewhart chart [Shewhart, 1925], Cumulative Sum (CUSUM) [Page, 1954], and Shiryaev-Roberts (SR) [Shiryaev, 1963]. For comprehensive and systematic reviews of parametric change-point detection, readers are referred to Basseville et al. [1993], Siegmund [2013], Tartakovsky et al. [2014], Xie et al. [2021].

In modern applications, especially those involving high-dimensional data settings, specifying the exact probability distribution can be challenging, necessitating non-parametric and distribution-free methods. Non-parametric kernel-based approaches do not require distributional assumptions, allow flexible kernel choices, and have gained significant attention due to their flexibility and wide applicability. Notably, the kernel Maximum Mean Discrepancy (MMD) for two-sample tests [Gretton et al., 2006, Smola et al., 2007, Gretton et al., 2012a, Muandet et al., 2017] has been extensively studied.

Literature on kernel-based change-point detection has focused on the offline setting, where the objective is detecting and locating change points retrospectively. Offline change-point detection procedures typically involve two-sample tests for samples with multiple candidate change-point locations. Notable examples of such procedures include the maximum Kernel Fisher Discriminant Ratio-based procedure [Harchaoui et al., 2008], the kernel MMD-based Scan B -procedure [Li et al., 2019], and a recent kernel-based scan procedure designed to enhance detection power in high-dimensional settings [Song and Chen, 2022].

Online change-point detection seeks to detect changes as soon as possible using sequential data. Existing online kernel-based change-point detection procedures are mainly the Shewhart chart-type, such as Li et al. [2019]. The Shewhart chart-type procedure differs from the CUSUM-type procedure, which relies on CUSUM recursion and is generally more sensitive to detecting small changes [Xie et al., 2021]. The CUSUM-type kernel procedure was rarely considered in the literature, possibly due to its higher computational and memory cost than Shewhart chart-type procedures. Recently, Flynn and Yoo [2019] presented a Kernel CUSUM procedure by replacing the likelihood ratio in the CUSUM recursion with the *linear-time* MMD statistic and derived crude bounds for both ARL and EDD. However, the linear-time MMD statistics used therein to achieve the recursive computation of the detection statistic

Table 1: A summary of existing online kernel change-point detection procedures.

Detection procedure type	Existing literature
Shewhart chart	Huang et al. [2014], Chang et al. [2019]; Li et al. [2019], Bouchikhi et al. [2019]; Cobb et al. [2022]
CUSUM	Flynn and Yoo [2019]

has a lower statistical detection power compared with the full MMD statistic considered in this paper. It remains challenging to apply full MMD statistics in the CUSUM procedure due to increased computational and memory costs as the time horizon expands and to analyze its theoretical properties, which we aim to tackle in this paper. Here, we present a summary of existing kernel-based online change-point detection methods in Table 1, and a more comprehensive literature survey can be found in Section 1.1.

In this paper, we present a kernel-based CUSUM procedure for online change-point detection, referred to as the *Online Kernel CUSUM*, which differs from the Shewhart chart-type procedures (e.g., the Scan B -procedure [Li et al., 2019]) in the search for the unknown change-point location, and leads to improved performance in detecting small changes. At each time step, the procedure forms a set of self-normalizing kernel test statistics, one for each candidate change-point location, takes the maximum over the detection statistics, and detects a change when the maximum exceeds a pre-specified threshold value. We find numerically accurate approximations for two standard performance metrics: the Average Run Length (ARL), which is useful for calibrating the procedure to control false alarms, and the Expected Detection Delay (EDD). The EDD analysis is essential for determining the optimal window length, but such analysis is not present in closely related prior works (e.g., the Scan B -procedure). Based on the ARL and EDD analysis, we establish the optimal window length, defined as the minimal samples needed to be kept in the memory for our procedure to achieve a similar performance as the oracle procedure with infinite memory, to be on the order of the logarithm of ARL, which interestingly matches the classic result for the window-limited Generalized Likelihood Ratio procedure [Lai, 1995]. Algorithmic-wise, we present a recursive implementation of our procedure to achieve a constant computational and memory cost at each time step, which is essential for online change-point detection. We demonstrate the performance gain of our proposed approach using simulation and real-data experiments.

1.1 Literature

Kernel methods in change-point detection. An early work on kernel change-point detection is [Harchaoui and Cappé \[2007\]](#) for offline multiple change-point estimation method, and the method was extended by [Arlot et al. \[2019\]](#) to handle an unknown number of change points via a model selection penalty. [Garreau and Arlot \[2018\]](#) performed non-asymptotic analysis to show the multiple change-point estimations by model selection [[Arlot et al., 2019](#)] can estimate the correct number of change-points with high probability and locate them at the optimal rate. The problem of calibrating detection procedures also exists for maximum Kernel Fisher Discriminant Ratio based approach [[Harchaoui et al., 2008](#)], where they applied the bootstrap re-sampling method to compute the detection threshold. In addition, [Bouchikhi et al. \[2019\]](#), [Ferrari et al. \[2023\]](#) considered a kernel density ratio [[Huang et al., 2006](#), [Nguyen et al., 2010](#)] based Shewhart chart-type method for online change-point detection.

Kernel MMD and its application in change-point detection. [Gretton et al. \[2006\]](#), [Smola et al. \[2007\]](#), [Gretton et al. \[2012a\]](#) consider a measure of discrepancy between distributions via the Reproducing Kernel Hilbert Space (RKHS) embedding of distributions that leads to the kernel MMD statistic, which can be linked back to the classic U-statistic [[Serfling, 2009](#)]. Since then, kernel MMD two-sample tests [[Li and Yuan, 2019](#), [Balasubramanian et al., 2021](#)] have become popular and have been applied in various settings, ranging from anomaly detection [[Zou et al., 2014](#)], model criticism and goodness-of-fit test [[Lloyd and Ghahramani, 2015](#)], robust hypothesis testing [[Sun and Zou, 2021](#)], as well as change-point detection.

There are various offline kernel MMD-based change-point detection: apart from the aforementioned work such as [Truong et al. \[2019\]](#) developed a greedy single change-point estimation procedure, [Jones et al. \[2021\]](#) developed a multiple change-point estimation method leveraging Nyström kernel approximation [[Williams and Seeger, 2000](#)] to achieve linear complexity.

Online kernel MMD-based change-point detection procedures typically test for changes between a window of reference data and a window of sequential data. Recently, there has been much effort focusing on kernel MMD-based Shewhart chart-type procedures, which consider fixed-window length scan statistics, such as Scan B -procedure [[Li et al., 2019](#)]. Other contributions include [Huang et al. \[2014\]](#), which considers the RKHS-based control chart for online change-point detection, using full MMD statistics computed using sequential data (it differs from the Scan B -procedure, which is a block-based MMD statistic to enable quick detection), and utilized bootstrap to calibrate the detection, [Chang et al. \[2019\]](#) that

leveraged neural network-based data-driven kernel selection [Gretton et al., 2012b] to boost detection power, Cobb et al. [2022] that considered a memory-less geometric distribution of the stopping time to control the false alarm rate and calibrated the detection via bootstrap. However, an issue with the fixed-length scanning window of Shewhart chart-type procedures is that they do not account for unknown change-point location, which may decrease the detection power; Cobb et al. [2022] indeed tackled this problem by considering a heuristic time-varying threshold without theoretical analysis.

2 Methodology

2.1 Preliminaries

Consider independent and identically distributed (i.i.d.) reference samples from the domain \mathcal{X} (usually taken to be \mathbb{R}^d) following an unknown pre-change distribution with density p :

$$X_1, \dots, X_M \stackrel{i.i.d.}{\sim} p.$$

At time t , we observe i.i.d. data Y_1, \dots, Y_t sequentially. The online change-point detection problem tests the null hypothesis

$$H_0 : Y_1, \dots, Y_t \stackrel{i.i.d.}{\sim} p,$$

against the alternative hypothesis

$$H_1 : \exists \kappa < t, Y_1, \dots, Y_\kappa \stackrel{i.i.d.}{\sim} p, Y_{\kappa+1}, \dots, Y_t \stackrel{i.i.d.}{\sim} q,$$

where q , distinct from p , is the density of an unknown post-change distribution and $\kappa > 0$ is the unknown change-point location. We aim to detect the change as soon as possible after it has occurred while controlling the false alarms.

Our notations are standard. Under the null hypothesis, we use \mathbb{P}_∞ and \mathbb{E}_∞ to denote the probability and expectation when there is no change. Under the alternative hypothesis, when there is a change at time κ , $\kappa = 0, 1, \dots$, we use \mathbb{P}_κ and \mathbb{E}_κ to denote the probability and expectation in this case. In particular, $\kappa = 0$ denotes an immediate change. We denote $\mathbf{1}_d = (1, \dots, 1)^\top \in \mathbb{R}^d$, $\mathbf{0}_d = (0, \dots, 0)^\top \in \mathbb{R}^d$ and $I_d \in \mathbb{R}^{d \times d}$ as the identity matrix, where superscript $^\top$ stands for the vector or matrix transpose. For integers $0 < m \leq n$, let $[m : n] = \{m, \dots, n\}$, and $[n] = \{1, \dots, n\}$. We denote $a \wedge b = \min\{a, b\}$, $a \vee b = \max\{a, b\}$ and

$(a)^+ = \max\{a, 0\}$. For asymptotic notations, we adopt standard definitions: $f(m) = o(g(m))$ means for all $c > 0$ there exists $k > 0$ such that $0 \leq f(m) < cg(m)$ for all $m \geq k$; $f(m) = \mathcal{O}(g(m))$ means there exist positive constants c and k , such that $0 \leq f(m) \leq cg(m)$ for all $m \geq k$; $f(m) \sim g(m)$ means there exist positive constants c and k , such that $0 \leq cg(m) \leq f(m)$ for all $m \geq k$ and at the same time $f(m) = \mathcal{O}(g(m))$.

2.2 Classic Parametric Procedures

Shewhart chart [Shewhart, 1925] uses a sliding window to compute detection statistics, which can be either parametric, e.g., based on likelihood ratio, or non-parametric. For the parametric approach, at time step t , the Shewhart chart uses the log-likelihood ratio of the most recent sequential observation Y_t as the detection statistic, i.e., $\log(q(Y_t)/p(Y_t))$. However, due to the sliding window approach, the Shewhart chart disregards the past sequential observations, and there can be an “information loss” that can lower the detection power (see, e.g., Xie et al. [2021]).

The likelihood-ratio based on CUSUM procedure [Page, 1954] assumes that densities p and q are both known. Given the sequential data Y_1, \dots, Y_t , the CUSUM procedure computes the cumulative log-likelihood ratio while taking the maximum with respect to the unknown change-point location, i.e.,

$$\begin{aligned} S_t &= \max_{1 \leq \kappa \leq t+1} \sum_{s=\kappa}^t \log \frac{q(Y_s)}{p(Y_s)} \\ &= \sum_{s=1}^t \log \frac{q(Y_s)}{p(Y_s)} - \min_{0 \leq \kappa \leq t} \sum_{s=1}^{\kappa} \log \frac{q(Y_s)}{p(Y_s)}. \end{aligned} \tag{1}$$

CUSUM procedure utilizes complete history information and is particularly popular for online change-point detection due to its recursive implementation:

$$S_t = \left(S_{t-1} + \log \frac{q(Y_t)}{p(Y_t)} \right)^+, \quad S_0 = 0. \tag{2}$$

The CUSUM procedure is defined as the first time t that the statistic S_t exceeds a pre-set threshold. Notably, Lorden [1971], Moustakides [1986] showed that the likelihood ratio based CUSUM enjoys optimality property.

When the post-change distribution has unknown parameters θ , the Generalized Likelihood

Ratio (GLR) procedure [Lorden, 1971, Siegmund and Venkatraman, 1995] is used:

$$\max_{1 \leq \kappa \leq t-1} \sup_{\theta \in \Theta} \sum_{s=\kappa}^t \log \frac{q(Y_s; \theta)}{p(Y_s)},$$

which involves maximum likelihood estimation of both change-point location κ and parameter θ . Although the inner supremum accounts for the unknown post-change distribution parameter, the GLR statistic loses the recursive implementation. To reduce the computational cost, a *window-limited* GLR (W-GLR) is adopted by restricting the search for the potential change-point to the most recent w data points, i.e., the outer maximization is over $\kappa \in [t - w : t - 1]$. The window length parameter w is crucial to the success of the W-GLR procedure, and Lai [1995] proved that, as $\gamma \rightarrow \infty$, the optimal window length under the Gaussian mean shift assumption is $w \sim \log \gamma$. According to Lai [2001], by choosing such a window length, “there is little loss of efficiency in reducing the computational complexity by the window-limited modification”.

2.3 Kernel MMD-Based Scan B -Procedure

Kernel-based statistics are popular for non-parametric two-sample tests of high-dimensional data (e.g., Gretton et al. [2012a]) due to their flexibility. Shewhart chart type of kernel-based online change-point detection procedure, Scan B , has been considered in [Li et al., 2019]. In the online Scan B -procedure, N *pre-change blocks* with equal block size B , denoted by $\mathbf{X}_B^{(i)}, i \in [N]$, are built by randomly sampling NB samples from the reference data X_1, \dots, X_M without replacement, assuming the reference sample size M is large enough such that $M > NB$. At time t , the *post-change block* consists of the most recent B sequential data, i.e., $\mathbf{Y}_B(t) = (Y_{t-B+1}, \dots, Y_t)$. The detection statistic is obtained by computing the unbiased MMD statistic between the post-change block and each pre-change block and taking their average:

$$Z_B(t) = \frac{\widehat{\mathcal{D}}_B(t)}{\sqrt{\text{Var}_\infty(\widehat{\mathcal{D}}_B(t))}}, \quad (3)$$

where $\text{Var}_\infty(\cdot)$ denotes the variance under H_0 and

$$\widehat{\mathcal{D}}_B(t) = \frac{1}{N} \sum_{i=1}^N \widehat{\mathcal{D}}(\mathbf{X}_B^{(i)}, \mathbf{Y}_B(t)). \quad (4)$$

For $\mathbf{X} = (X_1, \dots, X_B)$ and $\mathbf{Y} = (Y_1, \dots, Y_B)$, here we use the unbiased estimator of MMD [Gretton et al., 2012a]:

$$\begin{aligned} \widehat{\mathcal{D}}(\mathbf{X}, \mathbf{Y}) &= \frac{1}{B(B-1)} \sum_{i=1}^B \sum_{j \neq i}^B k(X_i, X_j) + \frac{1}{B(B-1)} \sum_{i=1}^B \sum_{j \neq i}^B k(Y_i, Y_j) \\ &\quad - \frac{2}{B(B-1)} \sum_{i=1}^B \sum_{j \neq i}^B k(X_i, Y_j) \\ &= \frac{1}{B(B-1)} \sum_{i=1}^B \sum_{j \neq i}^B h(X_i, X_j, Y_i, Y_j), \end{aligned} \tag{5}$$

where

$$h(x_1, x_2, y_1, y_2) = k(x_1, x_2) + k(y_1, y_2) - k(x_1, y_2) - k(x_2, y_1), \tag{6}$$

and $k(\cdot, \cdot)$ is the user-specified kernel function:

$$k(\cdot, \cdot) : \mathcal{X} \times \mathcal{X} \rightarrow \mathbb{R}.$$

Commonly used kernel functions include Gaussian radial basis function (RBF) $k(x, y) = \exp\{-\|x - y\|^2/r^2\}$, where $\|\cdot\|$ is the vector ℓ_2 norm and $r > 0$ is the bandwidth parameter.

Scan B -procedure uses one post-change block $\mathbf{Y}_B(t)$ in computing MMD with respect to all the reference blocks and only requires $\mathcal{O}(NB^2)$ computations. Since the block size B is typically held constant and N will depend on the reference sample size M , the Scan B -procedure achieves linear complexity, addressing the quadratic computational complexity issue in MMD statistics.

The normalizing constant, i.e., the standard deviation of $\widehat{\mathcal{D}}_B(t)$ under H_0 , has an analytic expression and thus can be estimated using the reference samples prior to the online implementation of the detection procedure.

Lemma 1 (Lemma 3.1 [Li et al., 2019]). Under H_0 , for block size $B \geq 2$ and the number of pre-change blocks $N > 0$, under H_0 , we have

$$\begin{aligned} \text{Var}_\infty(\widehat{\mathcal{D}}_B(t)) &= \frac{2(\mathbb{E}[h^2(X, X', Y, Y')] + (N-1)\text{Cov}[h(X, X', Y, Y'), h(X'', X''', Y, Y')])}{NB(B-1)}, \end{aligned} \tag{7}$$

where X, X', X'', X''', Y, Y' are i.i.d. random variables following p .

The online Scan B -procedure with block size B is defined by the first time t that $Z_B(t)$

exceeds a pre-set detection threshold. For brevity, we refer to the online Scan B -procedure as the Scan B -statistic or procedure, since this work does not consider the offline setting.

3 Proposed Detection Procedure

Inspired by the original form of recursive online CUSUM (1), we propose to consider a parallel set of Scan B -statistics $Z_B(t)$ in (3) with block size B taking values from $[2 : w]$ and take their maximum. For a pre-selected threshold b , the *online kernel CUSUM* procedure is defined via the following stopping time:

$$T_w = \inf \left\{ t : \max_{B \in [2:w]} Z_B(t) \geq b \right\}. \quad (8)$$

where w is the *window length* parameter.

The detection statistic in (8) can be computed recursively, which is crucial for online implementation: (a) Specifically, the computation of the MMD statistic involves evaluating the Gram matrix, which can be updated recursively as we receive sequential data. Such a recursive update with increasing time t was first considered in Li et al. [2019]. (b) The main difference between our CUSUM-type procedure and the Shewhart chart-type Scan B -procedure is the window-limited maximization with respect to $B \in [2 : w]$. Importantly, this additional window-limited maximization can be implemented in $\mathcal{O}(Nw^2)$ computations, ensuring that the overall computational and memory complexity of our procedure remains the same as that of Scan B -procedure with block size w . Moreover, since the Gram matrix can be updated recursively, the overall computational and memory complexity remains linear in sample size, and it does not grow with time, ensuring computational efficiency in practice. One can see the complete details of our detection procedure in Algorithm 1 and the graphical illustration of the recursive calculations in Figure 1.

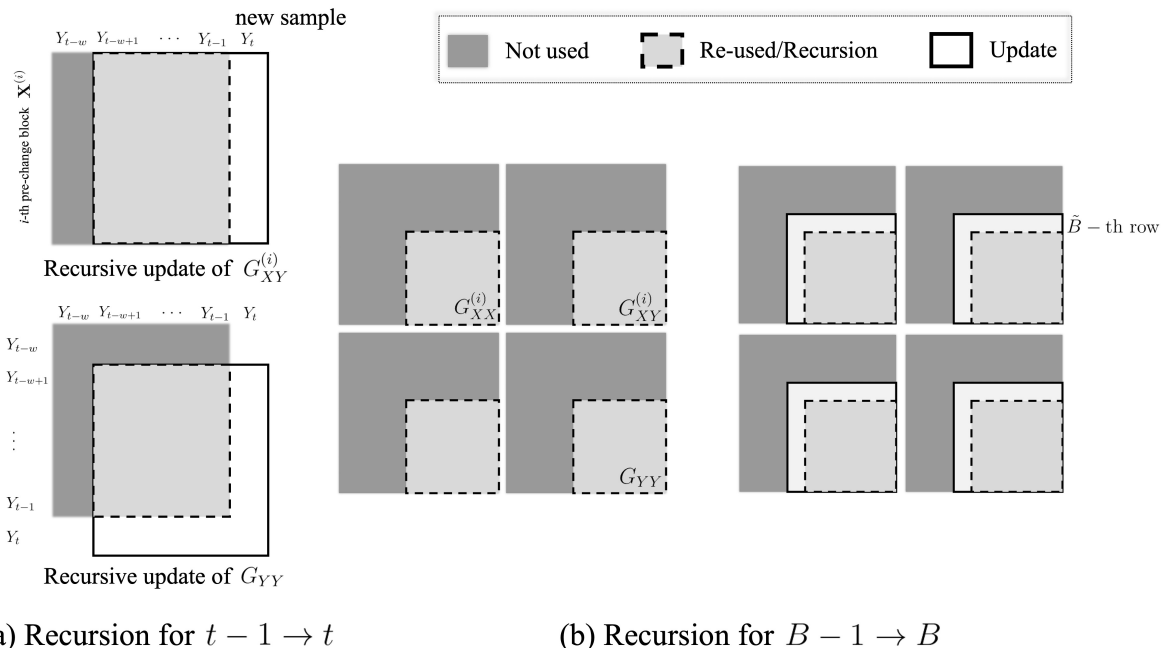


Figure 1: Graphical illustration of the recursive calculation: $G_{XX}^{(i)}$, $G_{XY}^{(i)}$ and G_{YY} denote the Gram metrics and $\tilde{B} = w - B + 1$; see definitions in Algorithm 1. The light gray part of the Gram matrix can be readily obtained from previous calculations, and only the white part needs to be updated (or re-calculated).

Compared to the Scan B -procedure, our proposed procedure offers improved performance by enhancing detection power under the same false alarm constraint, achieved by taking the maximum over detection statistics with different block sizes B . Since the change-point κ is unknown, the maximum is likely to be achieved for the block size B such that $[t - B + 1, t]$ contains all post-change samples. In contrast, the Scan B -procedure employs a fixed post-change block size and may include some pre-change samples in the post-change sample block, which can diminish its detection power. Maximizing the utilization of a small post-change sample size is crucial to detect the change as soon as possible after it occurs. Moreover, our proposed detection statistic has a constant expected increment value, facilitating the derivation of the analytic EDD approximation. However, the Scan B statistic includes varying post-change samples as it scans through the change-point over time, making it challenging to derive an analytic EDD approximation.

Figure 2 shows numerical evidence for the advantages of our proposed online kernel CUSUM over the Scan B -procedure, in which the mean trajectories over 100 independent trials are plotted; we highlight the mean \pm standard deviation region. Detailed experimental settings can be found in Section 5. Our detection statistic has a larger slope after the change-point than the Scan B -procedure, indicating a quicker detection. Additionally, both

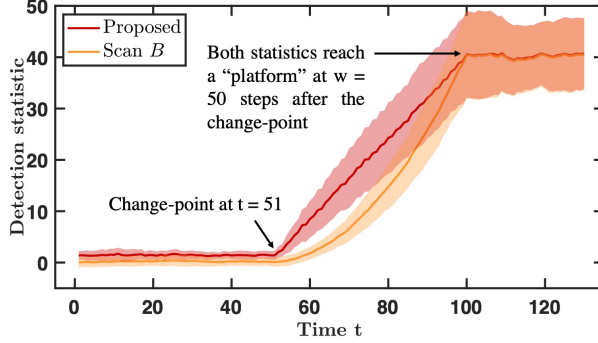


Figure 2: Trajectories of the mean (solid line) and standard deviation (shaded region) of our proposed and Scan B detection statistics over 100 independent trials. Change from $p = \mathcal{N}(\mathbf{0}_{20}, I_{20})$ to Gaussian mixture with $\mathcal{N}(\mathbf{0}_{20}, I_{20})$ w.p. 0.3 and $\mathcal{N}(\mathbf{0}_{20}, 4 I_{20})$ w.p. 0.7 occurs at $t = 51$.

statistics stop increasing after $w = 50$ steps from the change-point and plateau around similar values, which validates the necessity of choosing a large w according to (15) in our following EDD analysis to ensure the procedure stops with a moderate EDD.

3.1 Recursive Computation of Detection Statistic

For a matrix $G \in \mathbb{R}^{m \times n}$, $G(i_1 : i_2, j_1 : j_2)$ represents a slice of matrix G containing its i_1 -th to i_2 -th rows and j_1 -th to j_2 -th columns; in particular, when we want to include all rows (or columns) in this slice, we use “:” instead of “1 : m ” (or “1 : n ”). Similarly, for a vector $g \in \mathbb{R}^m$, $g(i : j)$ represents a slice of g , containing its i -th to j -th elements. In Algorithm 1, the recursive computation of detection statistics comes from two parts: a recursive update of Gram matrices (lines 5 – 8) and a recursive formulation to find the window-limited maximum (lines 9 – 13), which are direct benefits of CUSUM and closely resemble that of the original CUSUM (2).

3.2 Complexity Analysis

Even though the online update of Gram matrices only takes $\mathcal{O}(Nw)$ computational complexity, the whole procedure still takes $\mathcal{O}(Nw^2)$ computations to calculate the detection statistic in lines 9 – 13, which is the same with Scan B -procedure. To be precise, for fixed t , our detection procedure scans through $B \in [2 : w]$ to calculate the maximum of the Scan B -statistics, where the recursive update in line 12 only requires additional $\mathcal{O}(NB)$ computations and does not require additional memory to store those intermediate calculations; such a recursive computation results in $\mathcal{O}(N \sum_{B=2}^w B) = \mathcal{O}(Nw^2)$ total computations. We need to clarify

Algorithm 1 Online Kernel CUSUM

- 1: Initialization: estimate ρ (14) using historical data, take post-change block $\mathbf{Y} = \mathbf{Y}_w(t)$, and calculate the Gram matrices

$$G_{XX}^{(i)} = k(\mathbf{X}^{(i)}, \mathbf{X}^{(i)}), \quad G_{XY}^{(i)} = k(\mathbf{X}^{(i)}, \mathbf{Y}), \quad i = 1, \dots, N, \quad G_{YY} = k(\mathbf{Y}, \mathbf{Y})$$

- 2: **while** True **do**

- 3: receive sample Y_t

- 4: update post-change block:

$$\mathbf{Y}(1 : w - 1) \leftarrow \mathbf{Y}(2 : w), \quad \mathbf{Y}(w) \leftarrow Y_t$$

- 5: update Gram matrix G_{YY} :

$$\begin{aligned} G_{YY}(1 : w - 1, 1 : w - 1) &\leftarrow G_{YY}(2 : w, 2 : w), \\ G_{YY}(:, w) &\leftarrow k(\mathbf{Y}, Y_t), \quad G_{YY}(w, :) \leftarrow G_{YY}^T(:, w) \end{aligned}$$

- 6: **for** $i = 1, \dots, N$ **do**

- 7: update Gram matrix $G_{XY}^{(i)}$:

$$G_{XY}^{(i)}(:, 1 : w - 1) \leftarrow G_{XY}^{(i)}(:, 2 : w), \quad G_{XY}^{(i)}(:, w) \leftarrow k(\mathbf{X}^{(i)}, Y_t)$$

- 8: **end for**

- 9: calculate

$$\begin{aligned} z &= \sum_{i=1}^N G_{XX}^{(i)}(w - 1, w) + G_{YY}(w - 1, w) - 2G_{XY}^{(i)}(w - 1, w), \\ Z_t &= \frac{\rho}{N\sqrt{2}} z \end{aligned}$$

- 10: **for** $B = 3, \dots, w$ **do**

- 11: calculate $\tilde{B} = w - B + 1$

- 12: update

$$\begin{aligned} z &\leftarrow z + \sum_{i=1}^N \sum_{k=\tilde{B}+1}^w G_{XX}^{(i)}(\tilde{B}, k) + G_{YY}(\tilde{B}, k) - 2G_{XY}^{(i)}(\tilde{B}, k) \\ Z_t &\leftarrow \max \left\{ Z_t, \frac{\rho}{N\sqrt{B(B-1)}} z \right\} \end{aligned}$$

- 13: **end for**

- 14: **if** $Z_t > b$ **then**

- 15: raise an alarm, set $T_w = t$ and break

- 16: **end if**

- 17: **end while**
-

Table 2: Comparison of online change-point detection methods. Here, w is the window length parameter and N is the number of pre-change blocks.

	Assumptions	Computational Complexity	Memory
Shewhart chart	p and q are both known	$\mathcal{O}(1)$	–
CUSUM	p and q are both known	$\mathcal{O}(1)$	$\mathcal{O}(1)$
W-GLR	p is known and q has known form	$\mathcal{O}(w^2)$	$\mathcal{O}(w)$
Scan B	p and q are both unknown	$\mathcal{O}(Nw^2)$	$\mathcal{O}(Nw)$
Proposed	p and q are both unknown	$\mathcal{O}(Nw^2)$	$\mathcal{O}(Nw)$
Oracle	p and q are both unknown	$\mathcal{O}(Nt^2)$	$\mathcal{O}(Nt)$

that Algorithm 1 requires $\mathcal{O}(Nw^2)$ memory to store the Gram matrix. However, in theory, we can only use $\mathcal{O}(Nw)$ memory to store raw observations and re-compute the whole Gram matrix with $\mathcal{O}(Nw^2)$ computations at each time step. Table 2 provides a comparison among the Shewhart chart, CUSUM, W-GLR, Scan B , our proposed online kernel CUSUM, and its oracle variant (17).

4 Theoretical Properties

In this section, we derive analytic approximations for two standard performance metrics in online change-point detection [Xie and Siegmund, 2013]: the Average Run Length (ARL) (i.e., $\mathbb{E}_\infty[T_w]$, the expected stopping time when there is no change), and the Expected Detection Delay (EDD) (i.e., $\mathbb{E}_0[T_w]$, the expected stopping time when the change occurs immediately at $\kappa = 0$). Our ARL approximation is shown to be accurate numerically, enabling us to calibrate the detection procedure without relying on time-consuming Monte Carlo simulations. These results also allow us to establish the asymptotically optimal window length w^* in the same sense as that in Lai [1995].

4.1 Assumptions

We begin with the assumptions on the kernel. Consider the probability measure P (corresponding to the pre-change distribution) on a measurable space $(\mathcal{X}, \mathcal{B})$. For symmetric, positive semi-definite, and square-integrable (with respect to measure P) kernel function $k(\cdot, \cdot)$, Mercer’s theorem gives the following decomposition:

$$k(x, x') = \sum_{j=1}^{\infty} \lambda_j \varphi_j(x) \varphi_j(x'),$$

where the limit is in $L^2(p)$, $\lambda_1 \geq \lambda_2 \geq \dots \geq 0$ are eigenvalues of the integral operator induced by kernel k , and $\{\varphi_j(\cdot) : j \geq 1\}$ are the corresponding orthonormal eigenfunctions such that

$$\int_{\mathcal{X}} \varphi_j(x) \varphi_{j'}(x) dP(x) = \begin{cases} 1 & \text{if } j = j', \\ 0 & \text{otherwise.} \end{cases}$$

To avoid considering the meaningless zero kernel, we assume the largest eigenvalue is positive, i.e., $\lambda_1 > 0$. In addition, we further impose a technical assumption that all eigenfunctions are uniformly bounded, i.e.,

$$\sup_{j \geq 1} \|\varphi_j\|_{\infty} < \infty,$$

where $\|\varphi_j\|_{\infty} = \sup_{x \in \mathcal{X}} |\varphi_j(x)|$. This assumption ensures that the kernel $k(\cdot, \cdot)$ is uniformly bounded on domain $\mathcal{X} \times \mathcal{X}$, i.e., there exists a constant $K > 0$ such that

$$0 \leq k(x, y) \leq K, \quad \forall x, y \in \mathcal{X}. \quad (\text{A1})$$

Our approach does not impose any restrictions on the rank of the kernel function, meaning that the kernel does not necessarily need to be characteristic. For instance, on the domain $\mathcal{X} = \mathbb{R}^d$, the polynomial kernel function $k_{\ell}(x, y) = (x^{\text{T}}y + c)^{\ell}$ is finite-rank and cannot differentiate between probability distributions p and q if they have the same first ℓ -th order moments. To avoid such undesirable cases, we will impose an assumption on the post-change distribution to ensure that the change can be detected with our chosen kernel at the population level.

Next, we consider the assumption on the post-change distribution q . To ensure the change from p to q is detectable with a chosen kernel k , we require the population MMD to be positive. The (squared) population MMD, denoted by $\mathcal{D}(p, q)$, can be expressed as:

$$\begin{aligned} \mathcal{D}(p, q) &= \int_{\mathcal{X}} \int_{\mathcal{X}} k(x, x') (p - q)(x) (p - q)(x') dx dx' \\ &= \sum_{j=1}^{\infty} \lambda_j \left(\int_{\mathcal{X}} \varphi_j(x) (p(x) - q(x)) dx \right)^2. \end{aligned} \quad (9)$$

The *detectability assumption* on q is that, for pre-change distribution p and kernel k satisfying all aforementioned assumptions, there exists j such that $\lambda_j > 0$ and

$$a_j = \int_{\mathcal{X}} \varphi_j(x) (p(x) - q(x)) dx \neq 0. \quad (\text{A2})$$

Here, a_j represents the ‘‘projection’’ of the departure $p - q$ along the ‘‘direction’’ φ_j , and

Assumption (A2) ensures that

$$\mathcal{D}(p, q) = \sum_{j=1}^{\infty} \lambda_j a_j^2 > 0.$$

We want to remark that, if we assume that kernel k is universal, i.e., $\varphi_j(\cdot) : j \geq 1$ forms an orthonormal basis of $L^2(p)$, the kernel will be full-rank and characteristic, i.e., $\mathcal{D}(p, q) > 0$ when $p \neq q$. However, such an assumption is stronger than we need in the following analysis. Additionally, we want to mention that a characteristic kernel does not necessarily imply its universality unless the kernel is translation-invariant or radial; a more detailed discussion can be found in [Sriperumbudur et al. \[2011\]](#).

4.2 Average Run Length

Approximating ARL $\mathbb{E}_{\infty}[T_w]$ in closed-form requires studying the behaviors of extremes of random fields, and we use the techniques developed in [Siegmund et al. \[2010\]](#), [Yakir \[2013\]](#): (i) change-of-measure via exponential tilting, (ii) applying likelihood ratio identity to change the probability of interest into expectation, and (iii) invoking localization theorem. We obtain the ARL approximation as follows:

Lemma 2 (ARL approximation). As $b \rightarrow \infty$, an approximation to ARL for our proposed online kernel CUSUM procedure T_w (8) is given by:

$$\mathbb{E}_{\infty}[T_w] = \frac{\sqrt{2\pi}}{b} \left\{ \sum_{B=2}^w e^{\psi_B(\theta_B) - \theta_B b} \frac{(2B-1)}{B(B-1)} \nu \left(\theta_B \sqrt{\frac{2(2B-1)}{B(B-1)}} \right) \right\}^{-1} [1 + o(1)], \quad (10)$$

where $\psi_B(\cdot)$ is defined as:

$$\psi_B(\theta) = \sum_{n=1}^{\infty} \frac{\mathbb{E}_{\infty}[Z_B^n(t)]}{n!} \theta^n,$$

and θ_B is obtained via solving $\dot{\psi}_B(\theta_B) = b$. Moreover, the function $\nu(\cdot)$ can be approximated as (cf. [Siegmund et al. \[2007\]](#)):

$$\nu(\mu) \approx \frac{(2/\mu)(\Phi(\mu/2) - 0.5)}{(\mu/2)\Phi(\mu/2) + \phi(\mu/2)},$$

where $\phi(\cdot)$ and $\Phi(\cdot)$ are the probability density function and the cumulative distribution function of the standard normal distribution, respectively.

Proof can be found in Appendix B.

In practice, incorporating the information of the first two order moments information will suffice for ARL approximation, i.e.,

$$\psi_B(\theta_B) \approx \theta_B^2/2, \quad \theta_B \approx b, \quad (11)$$

since under the null hypothesis, the detection statistic has an expectation of zero, this gives us

$$\mathbb{E}_\infty[T_w] = \sqrt{2\pi} \frac{be^{b^2/2}}{w} [1 + o(1)]. \quad (12)$$

A detailed derivation of the approximation in (12) can be found in Appendix B.

To obtain a more precise ARL approximation, one approach would be to incorporate higher order moments while solving for θ_B using the equation $\psi_B(\theta_B) = b$. We use *skewness correction* to consider the third order moment $\mathbb{E}_\infty[Z_B^3(t)]$ in the following way:

$$\begin{aligned} \psi_B(\theta_B) &\approx \theta_B^2/2 + \mathbb{E}_\infty[Z_B^3(t)]\theta_B^3/6, \\ \theta_B &\approx \frac{-1 + \sqrt{1 + 2b\mathbb{E}_\infty[Z_B^3(t)]}}{\mathbb{E}_\infty[Z_B^3(t)]}. \end{aligned} \quad (13)$$

Similar to the second order moment, the third order moment $\mathbb{E}_\infty[Z_B^3(t)]$ can be pre-estimated using the reference data; see Lemma 5 in Appendix A.

To demonstrate the accuracy of our ARL approximation, we compare it with Monte Carlo simulation results for three types of pre-change distributions (i.e., Gaussian, Exponential, and Laplace distributions) in Figure 3. Our approximations are reasonably accurate for setting thresholds in all three cases after the skewness correction. In Appendix D, we theoretically show that considering only finite-order moments can lead to underestimating the threshold b as shown in Figure 3. In particular, note that Gaussian pre-change distribution p does not mean $Z_B(t)$ is Gaussian, and indeed, incorporating skewness correction improves the accuracy of the ARL approximation.

4.3 Expected Detection Delay

The difficulty in approximating the EDD $\mathbb{E}_0[T_w]$ arises from the form of the detection statistic, which is the maximum of highly correlated random variables. Consequently, one cannot directly apply Wald's identity to approximate the EDD; we take a non-asymptotic approach and use Azuma's concentration inequality (Lemma 7 in Appendix C) for martingales with

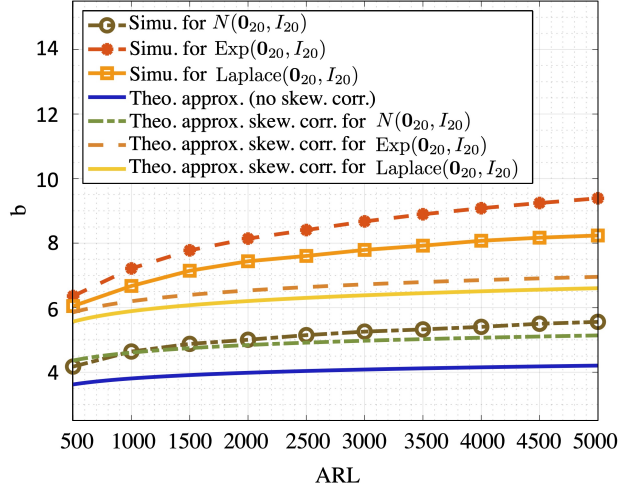


Figure 3: Comparison of the detection threshold b obtained by the Monte Carlo simulation (Simu.) and the theoretical approximation (with and without skewness correction) for a given ARL.

bounded differences to study the concentration of the Scan B -statistic. Denote

$$\rho = 2 \left(B(B-1) \text{Var}_\infty(\widehat{\mathcal{D}}_B(t)) \right)^{-1/2}, \quad (14)$$

where $\text{Var}_\infty(\widehat{\mathcal{D}}_B(t))$ is defined in (7). The EDD approximation is then given by:

Lemma 3 (EDD approximation). Under Assumptions (A1) and (A2), for window length

$$w \geq \frac{7b}{\rho \mathcal{D}(p, q)}, \quad (15)$$

and $N > 0$, as $b \rightarrow \infty$, the first-order approximation to EDD for online kernel CUSUM (8) is given by:

$$\mathbb{E}_0[T_w] = \frac{b}{\rho \mathcal{D}(p, q)} (1 + o(1)). \quad (16)$$

The proof of Lemma 3 can be found in Appendix C.

Remark 1 (Effect of pre-change block number N). The parameter N has a two-fold impact in our analysis: (1) the remainder term in (32) can be neglected only when N is sufficiently large. (2) it affects the EDD in (16) through the normalizing constant ρ in (14). To showcase the impact on EDD, let us consider the example in which the pre-change distribution is $\mathcal{N}(\mu \mathbf{1}_d, \sigma^2 I_d)$ and we use Gaussian RBF kernel with bandwidth r selected by the median heuristic [Schölkopf and Smola, 2002]. The Taylor expansion (see detailed derivations in

Appendix A) gives us:

$$0 < \mathbb{E} [h^2(X, X', Y, Y')] - \text{Cov} [h(X, X', Y, Y'), h(X'', X''', Y, Y')] = \mathcal{O}(1/d).$$

This implies that ρ monotonically increases with increasing N , i.e.,

$$\rho \rightarrow (\text{Cov} [h(X, X', Y, Y'), h(X'', X''', Y, Y')]/2)^{-1/2} \text{ as } N \rightarrow \infty,$$

meaning that larger N leads to smaller EDD according to (16). This finding agrees with the intuition: as N grows larger, the variance of $\widehat{\mathcal{D}}_B(t)$ reduces, which leads to a quicker detection (this is evidenced by Lemma 1 in Appendix A). Moreover, this shows ρ cannot increase unboundedly with increasing N .

4.4 Optimal Window Length

We now present the optimal window length parameter w due to ARL and EDD analysis by comparing our procedure with an *oracle procedure* using infinite past data up to time t . The stopping time of the oracle procedure with detection threshold $b > 0$ is defined as follows:

$$T_o = \inf \left\{ t : \max_{B \in [2:t]} Z_B(t) > b \right\}. \quad (17)$$

There is a trade-off between the computational and memory efficiency as well as the detection power: On one hand, larger w intuitively leads to smaller EDD, but the benefit diminishes as w further increases. On the other hand, the oracle procedure is computationally expensive as it involves $\mathcal{O}(t^2)$ computational complexity and $\mathcal{O}(t)$ memory up to time t , which is unsuitable for online settings. Thus, the fundamental question is: when holding ARL constant, what is the optimal window length w^* without sacrificing much performance?

Define a set of detection procedures with a constant ARL constraint $\gamma > 0$:

$$\mathcal{C}_\gamma = \{T : \mathbb{E}_\infty[T] \geq \gamma\}. \quad (18)$$

Following the optimality definition in Lai [1995], we are interested in

- (i) Choosing thresholds b 's for each procedure respectively to ensure $T_w, T_o \in \mathcal{C}_\gamma$, and
- (ii) for tolerance $\varepsilon > 0$, choosing an optimal window length w^* that incurs a ε -performance

loss, i.e.,

$$w^* = \min w, \quad \text{s.t. } 0 \leq \mathbb{E}_0[T_w] - \mathbb{E}_0[T_o] \leq \varepsilon. \quad (19)$$

We have the following result:

Theorem 1 (Optimal window length). Under Assumptions (A1) and (A2), for any $N > 0$, as $\gamma \rightarrow \infty$, when choosing $b \sim \log \gamma$, we have $T_w, T_o \in \mathcal{C}_\gamma$, and furthermore the optimal window length

$$w^* \sim \frac{6b}{\rho \mathcal{D}(p, q)} + \frac{512K^2 \log(3/\varepsilon)}{b^2 \left(\frac{N}{4} \wedge \frac{b}{\rho \mathcal{D}(p, q)} \right)}. \quad (20)$$

The main message from Theorem 1 is that the optimal window length is $w^* \sim \log \gamma$, as the first term in (20) dominates the second term when γ (and b) becomes large. While we only characterize the order of the optimal window length due to the complexity of our ARL approximation (10), the result $w^* \sim \log \gamma$ is informative to make a connection with classic parametric results. Specifically, our result is in a similar form as the classic result for window-limited GLR [Lai, 1995]. Furthermore, under the optimal choice w^* , the EDD of our proposed procedure will be:

$$\mathbb{E}_0[T_{w^*}] \sim \frac{\log \gamma}{\mathcal{D}(p, q)},$$

which closely resembles the EDD of the classic CUSUM procedure: $\mathcal{O}(\log \gamma / \text{KL}(q||p))$, where the denominator is the Kullback-Leibler divergence between two distributions q and p .

5 Numerical Experiments

In this section, we evaluate the performance of our proposed procedure. Specifically, we compare their EDDs for given ARLs to demonstrate the capability of our procedure to achieve quicker change detection. We also study different choices of hyperparameters, such as N and w to guide their selection in practice and validate our theoretical findings. The influence of hyperparameters is studied in Appendix E.1. Implementation is available online at https://github.com/SongWei-GT/online_kernel_cusum.

5.1 Simulations

To ensure that each detection procedure meets the given ARL constraint, we select the detection threshold b for each detection procedure separately via 1000 Monte Carlo trials. We then obtain the EDDs for each procedure as the average detection delays over another

1000 Monte Carlo trials with 10000 reference samples following p and 50 sequential samples following q . For our proposed procedure and Scan B -procedure, we choose $N = 15$, $w = 50$; we use Gaussian RBF kernel with bandwidth parameters selected via median heuristic. These choices are suggested by the experiments in Li et al. [2019] and our simulation result in Appendix E.1. We compare both procedures' EDDs (for given ARL) in Figure 4 under various settings, where we can observe improved performance (i.e., quicker change detection) of our proposed procedure.

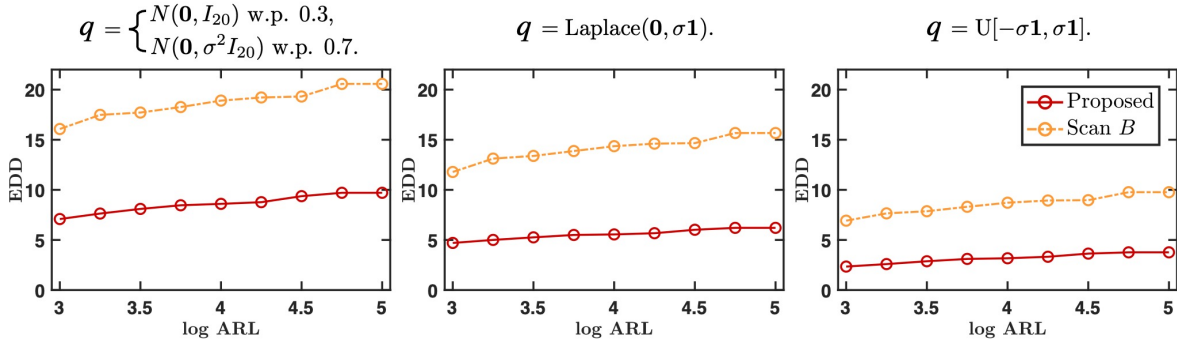


Figure 4: Comparison of EDD for given ARL between our proposed (red) and the Scan B (orange) detection procedures. In the x-axis, the ARL is in the base 10 logarithm. The pre-change distribution is $\mathcal{N}(\mathbf{0}_{20}, I_{20})$ and the post-change distribution q is specified on the top of each figure (with $\sigma = 2$).

In addition to the Scan B -procedure, we also compare with two other procedures: KCUSUM [Flynn and Yoo, 2019] using linear-time MMD statistic and the Hotelling's T^2 ; explanation of these procedures can be found in Appendix E.2. We plot the EDD against ARL for all four procedures in Figure 5, in which the absence of a dot indicates that the corresponding procedure fails to detect the change before the end of the simulated trajectory $t = 50$. Our method achieves the quickest detection for the same ARL, but also the most robust, capable of detecting even small changes that KCUSUM and parametric Hotelling's T^2 procedures fail to detect under the considered settings. In contrast, although KCUSUM occasionally achieves good detection performance, it tends to fail when the change is small or the ARL is large, indicating a lack of robustness. To further demonstrate the good performance of the proposed procedure, we present results under more scenarios in Appendix E.3.

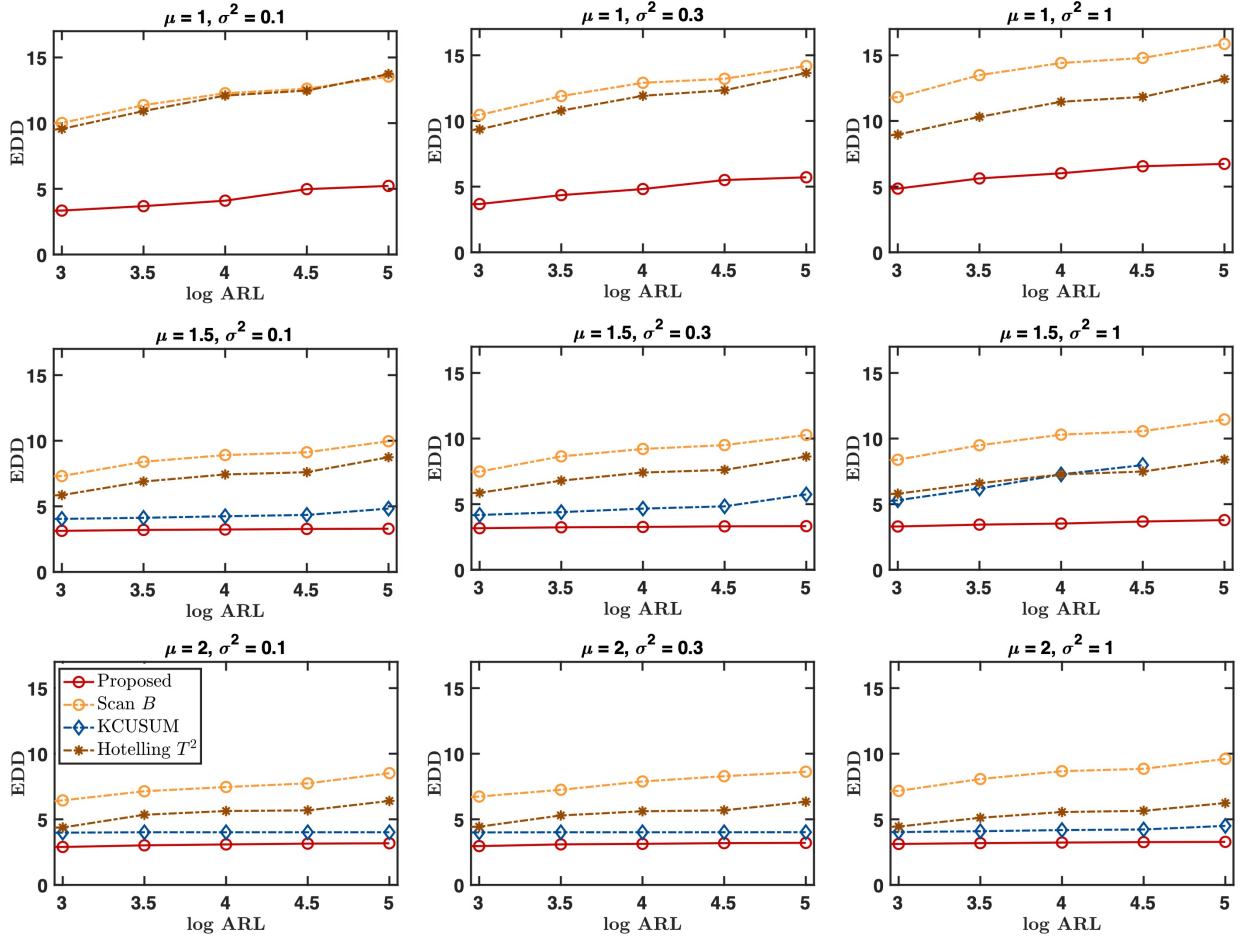


Figure 5: Comparison of EDD for our proposed (red), Scan B (orange), KCUSUM (blue), and Hotelling's T^2 (brown) procedures. The setting is: the pre-change distribution is $\mathcal{N}(\mathbf{0}_{20}, I_{20})$ and the post-change distribution is Gaussian mixture: $\mathcal{N}(\mathbf{0}_{20}, I_{20})$ w.p. 0.3; $\mathcal{N}(\mu \mathbf{1}_{20}, \sigma^2 I_{20})$ w.p. 0.7.

5.2 Real Experiments

In the last part, we demonstrate the performance of our proposed procedure on the Human Activity Sensing Consortium (HASC) dataset (available at <http://hasc.jp/hc2011>) and MNIST dataset [Watson and Wilson, 1992].

Human activity shift detection with HASC dataset. The HASC dataset contains 3-dimensional measurements of human activities collected by portable 3D accelerometers. To compare the performance of different detection procedures, we consider the change from walking to staying of human subject 101 and plot the detection statistics in Figure 6. The EDD and miss rate (out of 10 repeats) of each procedure are reported in Table 3. The detection threshold is chosen as the 80% quantile of the largest detection statistics over all repeats under H_0 (i.e., the post-change activity is the same as the pre-change activity) to control the false alarm rate at 0.2.

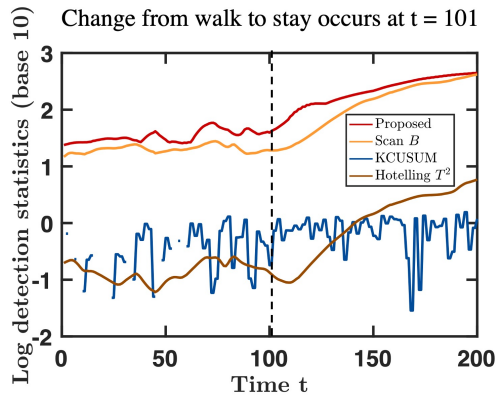


Figure 6: The trajectories of different detection statistics. Human subject 101 activity changes from walking to staying at time $t = 101$. The recursive update of KCUSUM (48) yields some zero statistics, which correspond to the “no value part” on the blue line.

Table 3: EDD (over successful detections) and miss (out of 10 repeats) of human activity change (from walking to other activities) detection for subject 101. The detection threshold is chosen as the 80% quantile of the maximum detection statistics under H_0 (i.e., the post-change activity is still walking).

Activity	Jog		Skip		Stay		Stair down		Stair up	
	EDD	Miss	EDD	Miss	EDD	Miss	EDD	Miss	EDD	Miss
Proposed	37.7	0	50.6	0	13	8	517.17	4	227.13	2
Scan B	73.7	0	82.4	0	72.2	0	329.71	3	207.33	7
KCUSUM	635	2	560.67	1	527.6	0	429.33	4	—	10
Hotelling T^2	77.6	5	242.8	5	26.5	8	114	5	44.67	7

As shown in Table 3, our procedure is robust and can successfully detect the change in almost all scenarios except for the change from walking to staying, where it misses most of the changes. However, as illustrated in Figure 6, our procedure performs well for some scenarios. Furthermore, our procedure achieves the quickest detection for changes from walking to jogging and skipping. Despite having the smallest EDD for changes to walking up and down the stairs, the parametric Hotelling’s T^2 procedure fails most of the time. These observations further validate the practical usefulness of our procedure. For completeness, we extend our experiment to the rest of the five human subjects and report the EDD and miss rates in Table 8 in Appendix E.4, which further demonstrates the excellent performance of our procedure for most scenarios. We also provide more details of the HASC dataset and the choices of hyperparameters in Appendix E.4.

Hand-written digits shift detection with MNIST dataset. The experiment considers detecting MNIST hand-written digits shift: we observe a sequence of digits that shift from one kind to another at some unknown time. The ambient dimension is 784 (28×28 -pixel image), but the intrinsic dimension is very low. The observations from pre- or post-change distribution are uniform random samples from a particular digit from $\{0, 1, \dots, 9\}$. EDD comparisons for the given ARL are presented in Figure 7. For each sub-figure, the detection threshold is obtained with 500 independent experiments with 3000 history data and 1000 sequential observations, both from the same pre-change distribution. Afterward, we perform another 500 independent experiments with 3000 history data and 100 sequential observations, where the sequential observations are from a post-change distribution, to obtain the average detection delay as the EDD. From figure 7, we can observe that the online kernel CUSUM can detect changes almost as fast as in the experiment with 20-dimensional simulated data in Section 5.1.

To make the detection task even more challenging, we center the data for each digit by subtracting its coordinate-wise average vector, ensuring zero mean for all digits’ data. We repeat the above experiment on this centered MNIST dataset and report the result in Table 4. In this setting, even though the EDDs become larger than that in Figure 7, the kernel method is still able to main detection power. Moreover, we can observe that in most cases our proposed method outperforms the Scan B -procedure and achieves quicker change detection. Meanwhile, in the rest cases where Scan B performs better, the EDDs of our proposed and Scan B -procedures are fairly close to each other, indicating very similar performance. Overall, this experiment verifies the good performance of our proposed procedure in a high dimensional setting.

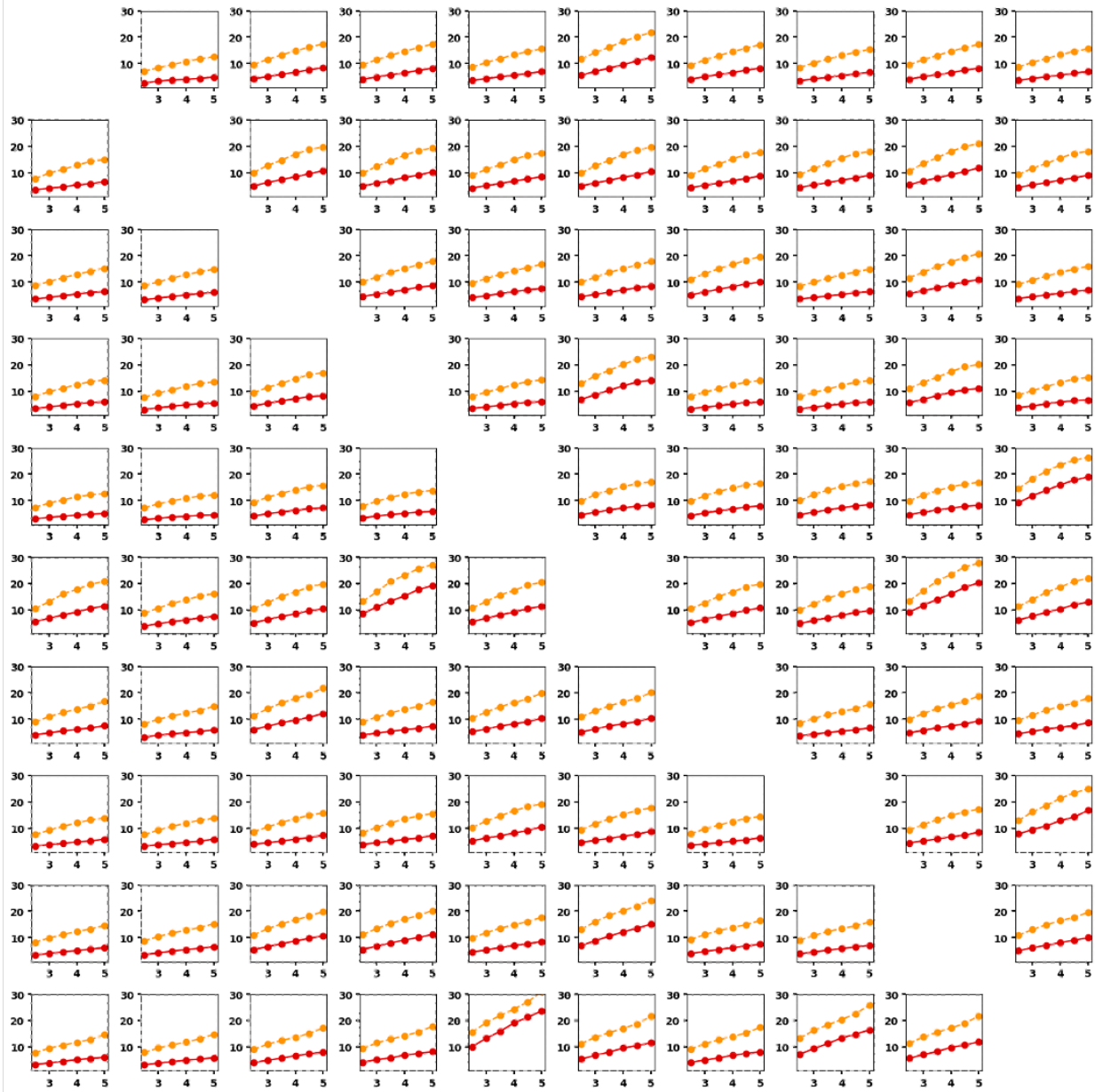


Figure 7: Comparison of EDD for given ARL between our proposed (red) and the Scan B (orange) detection procedures in detecting the transition of MNIST handwritten digits. In the 10-by-10 figure above, (i, j) -th sub-figure corresponds to the setting where the history data is uniform random samples from digit- i and the sequential observations are digit- j uniform random samples. In each sub-figure, x- and y-axes correspond to the log-ARL and EDD, respectively.

Table 4: EDD for target ARL $\gamma = 1000$. In the 10-by-10 table, the (i, j) -th entry contains EDDs (left: our proposed, right: the Scan B) under the setting where pre-change digit is i and post-change digit is j . In each entry, the smaller EDD is in a larger font, indicating the corresponding detection procedure is better under that specific setting; the entries where our proposed method outperforms Scan B are highlighted in bold fonts.

	0	1	2	3	4	5	6	7	8	9
0	-	31.04 _{30.31}	3.44 _{24.32}	3.68 _{25.22}	6.44 _{40.17}	9.48 _{26.94}	9.28 _{30.83}	16.26 _{49.01}	3.78 _{21.73}	11.64 _{47.18}
1	17.99 _{23.03}	-	19.18 _{23.81}	25.50 _{27.64}	31.63 _{30.73}	20.98 _{24.89}	25.88 _{27.88}	37.25 _{33.56}	25.10 _{27.37}	34.23 _{32.10}
2	29.03 _{46.57}	24.14 _{27.52}	-	10.44 _{30.95}	12.47 _{46.50}	25.51 _{47.05}	28.40 _{47.78}	29.69 _{46.93}	8.72 _{29.42}	28.42 _{47.55}
3	30.81 _{44.90}	27.12 _{29.56}	12.02 _{34.26}	-	10.80 _{35.16}	24.07 _{31.80}	26.40 _{45.41}	23.82 _{46.31}	7.87 _{19.91}	21.45 _{45.23}
4	37.42 _{40.39}	30.85 _{31.82}	27.27 _{48.39}	15.90 _{44.92}	-	32.74 _{47.76}	28.47 _{47.58}	17.78 _{31.63}	10.71 _{33.48}	13.63 _{16.30}
5	16.53 _{37.83}	30.93 _{29.46}	4.74 _{31.81}	4.67 _{13.90}	6.41 _{32.98}	-	12.13 _{34.06}	14.81 _{46.76}	2.64 _{10.94}	9.61 _{37.99}
6	20.68 _{44.07}	34.30 _{31.77}	10.38 _{47.44}	6.32 _{37.23}	4.69 _{30.83}	18.14 _{42.48}	-	16.63 _{49.15}	4.66 _{30.58}	12.23 _{46.41}
7	39.89 _{35.51}	39.60 _{34.91}	41.33 _{40.69}	19.34 _{47.91}	6.29 _{24.95}	37.31 _{41.23}	33.27 _{43.89}	-	16.33 _{46.44}	9.61 _{18.39}
8	30.63 _{46.34}	26.33 _{29.79}	16.17 _{34.58}	11.24 _{22.23}	10.19 _{27.69}	23.96 _{33.44}	27.29 _{44.77}	23.42 _{47.34}	-	18.12 _{38.59}
9	39.92 _{38.31}	35.87 _{34.49}	29.96 _{42.89}	12.08 _{45.15}	3.58 _{7.44}	28.91 _{45.68}	25.96 _{45.47}	9.77 _{19.13}	8.50 _{33.95}	-

6 Conclusion and Discussions

We presented an online kernel CUSUM procedure for change-point detection to overcome the limitations of existing Shewhart chart-type procedures, such as the Scan B -procedure, and boost the detection power from the linear-time kernel detection statistic, such as Flynn and Yoo [2019]. We present accurate theoretical approximations to two standard performance metrics, the ARL and EDD, from which we establish the optimal window length to be logarithmic in ARL, analogous to the classical parametric results. We validate the effectiveness of our procedure through extensive numerical experiments, demonstrating its superior performance compared to various existing procedures. Our findings contribute to the non-parametric change-point detection literature, providing a practical and robust method for detecting changes in sequential data.

A future direction is to study the dependence of the performance on the data dimension and structure and see how to extend existing results for fixed sample two-sample tests: for instance, when the data comes from high-dimensional isotropic Gaussian distribution, the kernel method has a curse of dimensionality, as the population MMD drops to zero exponentially fast as the dimension increases [Ramdas et al., 2015, Reddi et al., 2015]; and when data has an intrinsically low-dimensional structure such as manifold structures (many high-dimensional data including the commonly studied MNIST handwritten digits have this property), the MMD two-sample test has no curse-of-dimensionality [Cheng and Xie, 2023].

Acknowledgement

This work is partially supported by an NSF CAREER CCF-1650913, and NSF DMS-2134037, CMMI-2015787, DMS-1938106, and DMS-1830210.

References

- Sylvain Arlot, Alain Celisse, and Zaid Harchaoui. A kernel multiple change-point algorithm via model selection. *Journal of Machine Learning Research*, 20(162), 2019.
- Richard Arratia, Larry Goldstein, and Louis Gordon. Two moments suffice for poisson approximations: the chen-stein method. *The Annals of Probability*, pages 9–25, 1989.
- Krishnakumar Balasubramanian, Tong Li, and Ming Yuan. On the optimality of kernel-embedding based goodness-of-fit tests. *Journal of Machine Learning Research*, 22(1), 2021.
- Michele Basseville, Igor V Nikiforov, et al. *Detection of abrupt changes: theory and application*, volume 104. Prentice hall Englewood Cliffs, 1993.
- Ikram Bouchikhi, André Ferrari, Cédric Richard, Anthony Bourrier, and Marc Bernot. Kernel based online change point detection. In *2019 27th European Signal Processing Conference (EUSIPCO)*, pages 1–5. IEEE, 2019.
- Wei-Cheng Chang, Chun-Liang Li, Yiming Yang, and Barnabás Póczos. Kernel change-point detection with auxiliary deep generative models. *arXiv preprint arXiv:1901.06077*, 2019.
- Xiuyuan Cheng and Yao Xie. Kernel mmd two-sample tests for manifold data. *Bernoulli*, 2023.
- Oliver Cobb, Arnaud Van Looveren, and Janis Klaise. Sequential multivariate change detection with calibrated and memoryless false detection rates. In *International Conference on Artificial Intelligence and Statistics*, pages 226–239. PMLR, 2022.
- André Ferrari, Cédric Richard, Anthony Bourrier, and Ikram Bouchikhi. Online change-point detection with kernels. *Pattern Recognition*, 133:109022, 2023.
- Thomas Flynn and Shinjae Yoo. Change detection with the kernel cumulative sum algorithm. In *2019 IEEE 58th Conference on Decision and Control (CDC)*, pages 6092–6099. IEEE, 2019.

- Damien Garreau and Sylvain Arlot. Consistent change-point detection with kernels. *Electronic Journal of Statistics*, 12(2):4440–4486, 2018.
- Arthur Gretton, Karsten Borgwardt, Malte Rasch, Bernhard Schölkopf, and Alex Smola. A kernel method for the two-sample-problem. *Advances in Neural Information Processing Systems*, 19:513–520, 2006.
- Arthur Gretton, Karsten M Borgwardt, Malte J Rasch, Bernhard Schölkopf, and Alexander Smola. A kernel two-sample test. *Journal of Machine Learning Research*, 13(1):723–773, 2012a.
- Arthur Gretton, Dino Sejdinovic, Heiko Strathmann, Sivaraman Balakrishnan, Massimiliano Pontil, Kenji Fukumizu, and Bharath K Sriperumbudur. Optimal kernel choice for large-scale two-sample tests. *Advances in Neural Information Processing Systems*, 25, 2012b.
- Zaid Harchaoui and Olivier Cappé. Retrospective mutiple change-point estimation with kernels. In *2007 IEEE/SP 14th Workshop on Statistical Signal Processing*, pages 768–772. IEEE, 2007.
- Zaid Harchaoui, Eric Moulines, and Francis Bach. Kernel change-point analysis. *Advances in Neural Information Processing Systems*, 21, 2008.
- Wassily Hoeffding. Probability inequalities for sums of bounded random variables. In *The collected works of Wassily Hoeffding*, pages 409–426. Springer, 1994.
- Jiayuan Huang, Arthur Gretton, Karsten Borgwardt, Bernhard Schölkopf, and Alex Smola. Correcting sample selection bias by unlabeled data. *Advances in Neural Information Processing Systems*, 19:601–608, 2006.
- Shuai Huang, Zhenyu Kong, and Wenzhen Huang. High-dimensional process monitoring and change point detection using embedding distributions in reproducing kernel hilbert space. *IIE Transactions*, 46(10):999–1016, 2014.
- Corinne Jones, Sophie Clayton, François Ribalet, E Virginia Armbrust, and Zaid Harchaoui. A kernel-based change detection method to map shifts in phytoplankton communities measured by flow cytometry. *Methods in Ecology and Evolution*, 12(9):1687–1698, 2021.
- Tze Leung Lai. Sequential changepoint detection in quality control and dynamical systems. *Journal of the Royal Statistical Society: Series B (Methodological)*, 57(4):613–644, 1995.

- Tze Leung Lai. Sequential analysis: some classical problems and new challenges. *Statistica Sinica*, pages 303–351, 2001.
- Shuang Li, Yao Xie, Hanjun Dai, and Le Song. Scan B-statistic for kernel change-point detection. *Sequential Analysis*, 38(4):503–544, 2019.
- Tong Li and Ming Yuan. On the optimality of gaussian kernel based nonparametric tests against smooth alternatives. *arXiv preprint arXiv:1909.03302*, 2019.
- James R Lloyd and Zoubin Ghahramani. Statistical model criticism using kernel two sample tests. *Advances in Neural Information Processing Systems*, 28, 2015.
- Gary Lorden. Procedures for reacting to a change in distribution. *The Annals of Mathematical Statistics*, pages 1897–1908, 1971.
- George V Moustakides. Optimal stopping times for detecting changes in distributions. *The Annals of Statistics*, 14(4):1379–1387, 1986.
- Krikamol Muandet, Kenji Fukumizu, Bharath Sriperumbudur, Bernhard Schölkopf, et al. Kernel mean embedding of distributions: A review and beyond. *Foundations and Trends® in Machine Learning*, 10(1-2):1–141, 2017.
- XuanLong Nguyen, Martin J Wainwright, and Michael I Jordan. Estimating divergence functionals and the likelihood ratio by convex risk minimization. *IEEE Transactions on Information Theory*, 56(11):5847–5861, 2010.
- Ewan S Page. Continuous inspection schemes. *Biometrika*, 41(1/2):100–115, 1954.
- Aaditya Ramdas, Sashank Jakkam Reddi, Barnabás Póczos, Aarti Singh, and Larry Wasserman. On the decreasing power of kernel and distance based nonparametric hypothesis tests in high dimensions. In *Proceedings of the AAAI Conference on Artificial Intelligence*, volume 29, 2015.
- Sashank Reddi, Aaditya Ramdas, Barnabás Póczos, Aarti Singh, and Larry Wasserman. On the high dimensional power of a linear-time two sample test under mean-shift alternatives. In *International Conference on Artificial Intelligence and Statistics*, pages 772–780. PMLR, 2015.
- Bernhard Schölkopf and Alexander J Smola. *Learning with kernels: support vector machines, regularization, optimization, and beyond*. MIT press, 2002.

- Robert J Serfling. *Approximation theorems of mathematical statistics*. John Wiley & Sons, 2009.
- Walter A Shewhart. The application of statistics as an aid in maintaining quality of a manufactured product. *Journal of the American Statistical Association*, 20(152):546–548, 1925.
- Albert N Shiryaev. On optimum methods in quickest detection problems. *Theory of Probability & Its Applications*, 8(1):22–46, 1963.
- David Siegmund. *Sequential analysis: tests and confidence intervals*. Springer Science & Business Media, 2013.
- David Siegmund and ES Venkatraman. Using the generalized likelihood ratio statistic for sequential detection of a change-point. *The Annals of Statistics*, pages 255–271, 1995.
- David Siegmund, Benjamin Yakir, et al. *The statistics of gene mapping*, volume 1. Springer, 2007.
- David Siegmund, Benjamin Yakir, and Nancy Zhang. Tail approximations for maxima of random fields by likelihood ratio transformations. *Sequential Analysis*, 29(3):245–262, 2010.
- Alex Smola, Arthur Gretton, Le Song, and Bernhard Schölkopf. A hilbert space embedding for distributions. In *International Conference on Algorithmic Learning Theory*, pages 13–31. Springer, 2007.
- Hoseung Song and Hao Chen. New kernel-based change-point detection. *arXiv preprint arXiv:2206.01853*, 2022.
- Bharath K Sriperumbudur, Kenji Fukumizu, and Gert RG Lanckriet. Universality, characteristic kernels and rkhs embedding of measures. *Journal of Machine Learning Research*, 12(7), 2011.
- Zhongchang Sun and Shaofeng Zou. A data-driven approach to robust hypothesis testing using kernel mmd uncertainty sets. In *2021 IEEE International Symposium on Information Theory (ISIT)*, pages 3056–3061. IEEE, 2021.
- Alexander Tartakovsky, Igor Nikiforov, and Michele Basseville. *Sequential analysis: Hypothesis testing and changepoint detection*. CRC Press, 2014.

- Charles Truong, Laurent Oudre, and Nicolas Vayatis. Greedy kernel change-point detection. *IEEE Transactions on Signal Processing*, 67(24):6204–6214, 2019.
- Craig I Watson and Charles L Wilson. Nist special database 4. *Fingerprint Database, National Institute of Standards and Technology*, 17(77):5, 1992.
- Christopher Williams and Matthias Seeger. Using the nyström method to speed up kernel machines. *Advances in Neural Information Processing Systems*, 13, 2000.
- Liyan Xie and Yao Xie. Sequential change detection by optimal weighted ℓ_2 divergence. *IEEE Journal on Selected Areas in Information Theory*, 2(2):747–761, 2021.
- Liyan Xie, Shaofeng Zou, Yao Xie, and Venugopal V Veeravalli. Sequential (quickest) change detection: Classical results and new directions. *IEEE Journal on Selected Areas in Information Theory*, 2(2):494–514, 2021.
- Yao Xie and David Siegmund. Sequential multi-sensor change-point detection. *The Annals of Statistics*, 41(2):670–692, 2013.
- Benjamin Yakir. *Extremes in random fields: A theory and its applications*. John Wiley & Sons, 2013.
- Wojciech Zaremba, Arthur Gretton, and Matthew Blaschko. B-test: A non-parametric, low variance kernel two-sample test. *Advances in Neural Information Processing Systems*, 26: 755–763, 2013.
- Shaofeng Zou, Yingbin Liang, H Vincent Poor, and Xinghua Shi. Nonparametric detection of anomalous data via kernel mean embedding. *arXiv preprint arXiv:1405.2294*, 2014.

Appendix of Online Kernel CUSUM for Change-Point Detection

Table of Contents

A	Moments of the Scan B-Statistic	32
B	Proof of Lemma 2	35
C	Proof of Lemma 3	38
D	Proof of Theorem 1	52
E	Additional Experimental Results	57
E.1	Study on the Hyperparameter Choices	57
E.2	Benchmark Procedures	61
E.3	EDD against ARL Comparison under More Settings	65
E.4	Real Example: HASC Dataset	65

A Moments of the Scan B -Statistic

Derivations in Remark 1. For notational simplicity, we denote

$$\begin{aligned} C_1 &= \mathbb{E} [h^2(X, X', Y, Y')], \\ C_2 &= \text{Cov} [h(X, X', Y, Y'), h(X'', X''', Y, Y')], \end{aligned} \tag{21}$$

where X, X', X'', X''', Y, Y' are i.i.d. random variables following p . By calculation, we have

$$C_1 - C_2 = \mathbb{E}[k^2(X, X')] - (\mathbb{E}[k(X, X')])^2 - 4(\mathbb{E}[k(X, X')k(X, Y)] - \mathbb{E}[k(X, X')k(X'', Y)]).$$

When we choose Gaussian RBF kernel with bandwidth parameter $r > 0$ and consider $p = \mathcal{N}(\mu \mathbf{1}_d, \sigma^2 I_d)$, we can evaluate the above quantity in closed-form. For notational simplicity, we denote

$$\begin{aligned} \tilde{r}_0 &= \left(\frac{r^2}{4\sigma^2 + r^2} \right)^{d/2}, \\ \tilde{r}_1 &= \left(1 - \frac{4\sigma^4}{(2\sigma^2 + r^2)^2} \right)^{d/2}, \\ \tilde{r}_2 &= \left(1 - \frac{3\sigma^4}{(3\sigma^2 + r^2)(\sigma^2 + r^2)} \right)^{d/2}. \end{aligned}$$

Then, we have

$$C_1 - C_2 = \tilde{r}_0 (1 - \tilde{r}_1 - 4\tilde{r}_2 + 4\tilde{r}_1) = \tilde{r}_0 (1 + 3\tilde{r}_1 - 4\tilde{r}_2).$$

We can see the problem boils down to evaluating $1 + 3\tilde{r}_1 - 4\tilde{r}_2$. When we use median heuristic to select kernel bandwidth, we will have $r^2 \sim d\sigma^2$. We plug it in $1 + 3\tilde{r}_1 - 4\tilde{r}_2$ and we will have $1 + 3\tilde{r}_1 - 4\tilde{r}_2$ approximated as follows:

$$1 + 3 \left(1 - \frac{3}{(3+d)(1+d)} \right)^{d/2} - 4 \left(1 - \frac{4}{(2+d)^2} \right)^{d/2}.$$

On one hand, we know $(1 + 1/d^2)^d \sim \exp\{1/d\} \rightarrow 1$ as $d \rightarrow \infty$. On the other hand, for relatively small d , we can calculate its value in Figure 8.

As we can see in Figure 8, the quantity $C_1 - C_2$ will be positive at least for d up to 1000. Since we also observe a monotonic decreasing trend, we conjecture that this quantity will always be positive. In fact, this can be theoretically proved. By Taylor expansion with

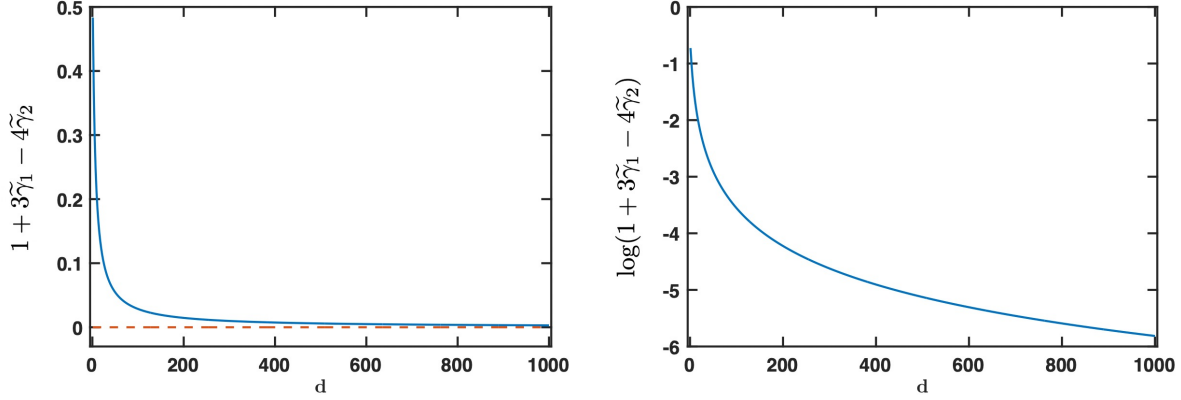


Figure 8: Numerical evaluation of $1 + 3\tilde{\gamma}_1 - 4\tilde{\gamma}_2$ up to $d = 1000$ when we take $r^2 = d\sigma^2$. We plot its raw value and its logarithm in the left and right panels, respectively.

Lagrange remainder, we will have

$$1 + 3\tilde{r}_1 - 4\tilde{r}_2 \geq 1 + 3 \exp\{-2d\sigma^4/r^4\} - 4 \exp\{-3d\sigma^4/(2r^4)\} - \frac{8d\sigma^6}{r^6} \exp\{2d\sigma^6/r^6\}.$$

Therefore, if we apply Taylor expansion and only keep the leading term, as long as

$$\sigma^2 = \mathcal{O}(r^2/\sqrt{d}), \quad (22)$$

we will have

$$1 + 3 \exp\{-2d\sigma^4/r^4\} - 4 \exp\{-3d\sigma^4/(2r^4)\} - \frac{8d\sigma^6}{r^6} \exp\{2d\sigma^6/r^6\} = \frac{3d\sigma^4}{2r^4}(1 + o(1)).$$

As we can see, median heuristic clearly satisfies condition (22). We can not only verify $1 + 3\tilde{r}_1 - 4\tilde{r}_2 \geq 0$ for large enough d , but also show the rate (at which it decays to zero) is $\mathcal{O}(1/d)$.

Lemma 4 (Covariance structure of $\widehat{\mathcal{D}}_B(t)$ under H_0). Under H_0 , for the un-normalized statistic $\widehat{\mathcal{D}}_B(t)$ (4), for block sizes $B_1, B_2 \geq 2$ and non-negative integer s , at time steps t and $t + s$, the covariance is as follows:

$$\text{Cov} \left(\widehat{\mathcal{D}}_{B_1}(t), \widehat{\mathcal{D}}_{B_2}(t + s) \right) = C_2 \binom{\ell}{2} / \binom{B_1}{2} \binom{B_2}{2},$$

where

$$\ell = \begin{cases} 0 & , \text{ if } B_2 - s < 0; \\ B_2 - s & , \text{ if } 0 \leq B_2 - s < B_1; \\ B_1 & , \text{ otherwise,} \end{cases}$$

and C_2 is defined in (21).

Proof. Notice that ℓ represents the length of overlap between $\widehat{\mathcal{D}}_{B_1}(t)$ and $\widehat{\mathcal{D}}_{B_2}(t+s)$. By Lemma B.2 [Li et al., 2019] and notice that $\widehat{\mathcal{D}}_{B_1}(t)$ and $\widehat{\mathcal{D}}_{B_2}(t+s)$ have different normalizing factors, we complete the proof. \square

Lemma 5 (Lemma 6.1 [Li et al., 2019]). Given block size $B \geq 2$ and the number of blocks N , under H_0 , the third order moment of $\widehat{\mathcal{D}}_B(t)$ (4) has an analytic expression as follows:

$$\begin{aligned} & \mathbb{E}_\infty \left[(\widehat{\mathcal{D}}_B(t))^3 \right] \\ &= \frac{8(B-2)}{B^2(B-1)^2} \left\{ \frac{1}{N^2} \mathbb{E} [h(X, X', Y, Y') h(X', X'', Y', Y'') h(X'', X, Y'', Y)] \right. \\ & \quad + \frac{3(N-1)}{N^2} \mathbb{E} [h(X, X', Y, Y') h(X', X'', Y', Y'') h(X''', X''', Y'', Y)] \\ & \quad \left. + \frac{(N-1)(N-2)}{N^2} \mathbb{E} [h(X, X', Y, Y') h(X'', X''', Y', Y'') h(X''', X''', Y'', Y)] \right\} \\ & \quad + \frac{4}{B^2(B-1)^2} \left\{ \frac{1}{N^2} \mathbb{E} [h(X, X', Y, Y')^3] \right. \\ & \quad + \frac{3(N-1)}{N^2} \mathbb{E} [h(X, X', Y, Y')^2 h(X'', X''', Y, Y')] \\ & \quad \left. + \frac{(N-1)(N-2)}{N^2} \mathbb{E} [h(X, X', Y, Y') h(X'', X''', Y, Y') h(X''', X''', Y, Y')] \right\}, \end{aligned}$$

where $X, X', X'', X''', X''', X''', Y, Y', Y''$ are all i.i.d. random variables following p .

The constant $\mathbb{E}_\infty[Z_B^3(t)] = \mathbb{E}_\infty[(\widehat{\mathcal{D}}_B(t))^3] \text{Var}(\widehat{\mathcal{D}}_B(t))^{-3/2}$ can be pre-calculated together with the constants in Lemma 1.

Lastly, we evaluate the moment of Scan B -statistic (3) under H_1 as follows:

Lemma 6 (Mean of $Z_B(t)$ under the alternative). Under H_1 , assume change occurs at time step 0, at time step $t < w$, the expectation of the Scan B -statistic (3) $\mu_B(t) = \mathbb{E}_0[Z_B(t)]$ has

the following explicit expression:

$$\begin{aligned}\mu_B(t) &= \rho \mathcal{D}(p, q) \sqrt{B(B-1)}, & B \in [2 : t], \\ \mu_B(t) &= \rho \mathcal{D}(p, q) \frac{t(t-1)}{\sqrt{B(B-1)}}, & B \in [t+1 : w],\end{aligned}$$

where constant ρ is defined in (14).

Proof. We can observe that when change occurs at $t = 0$, the most recent t samples will be post-change samples. Therefore, when $B > t$, the post-change block will also contain pre-change samples. Notice that $\mathcal{D}(p, p) = 0$ (see, e.g., Lemma 4 in Gretton et al. [2012a]). Then it reduces to a simple evaluation of the expectation (it is simple because the expectation is linear). We omit further detailed derivations and conclude the proof. \square

B Proof of Lemma 2

Under H_0 , the event that the statistic crosses the threshold b is rare. Therefore, as $b \rightarrow \infty$, for large enough m such that

$$\frac{\log b}{wm} \rightarrow 0, \quad \frac{wmb}{e^{b^2/2}} \rightarrow 0, \quad (23)$$

the null distribution of T_w can be approximated via the following exponential distribution with parameter λ :

$$\mathbb{P}_\infty(T_w \leq m) = \mathbb{P}_\infty\left(\max_{t \in [m]} \max_{B \in [2:w]} Z_B(t) \geq b\right) \approx 1 - \exp\{-\lambda m\} \approx \lambda m. \quad (24)$$

The above result can be derived using Poisson approximation technique (see, e.g., Theorem 1 [Arratia et al., 1989] and Appendix D [Li et al., 2019]). Intuitively, the interarrival time of the first rare event will follow an exponential limiting distribution. More precise statements as well as their detailed proof regarding the above exponential approximation can be found in Appendix D in Li et al. [2019] and we omit further technical details here.

One difference on of our exponential approximation from that of Li et al. [2019] is that they only require

$$\frac{\log b}{m} \rightarrow 0, \quad \frac{mb}{e^{b^2/2}} \rightarrow 0. \quad (25)$$

By comparing condition (23) and the above condition (25), we know that we cannot afford exponentially large w with respect to b . Nevertheless, on one hand, window length w is held constant in practice, which satisfies condition (23) automatically; on the other hand, we will

see in the following EDD analysis we only need $w \sim b$, which again satisfies condition (23).

Equation (24) tells us that the problem of approximating $\mathbb{E}_\infty[T_w]$ reduces to studying the extremes of random field $\{Z_B(t)\}$ with parameter (t, B) , which can be solved by determining the parameter λ of the limiting exponential distribution. To achieve this goal, a popular method is described in Section 4.2 (see steps (i), (ii), (iii) therein). A very clear and detailed instruction on how to prove the ARL approximation can be found in Appendices C and D [Li et al., 2019]. Here, we sketch the proof of Lemma 2 as follows:

Proof Sketch of Lemma 2. We give high-level ideas in each step described in Section 4.2. Moreover, we highlight the difference from the proof in Li et al. [2019] as follows:

- (i) We usually make use of log moment generating function $\psi_B(\theta) = \log \mathbb{E}_\infty[e^{\theta Z_B(t)}]$ and the new measure is defined as

$$dP_B = \exp\{\theta_B Z_B(t) - \psi_B(\theta_B)\} d\mathbb{P}_\infty.$$

Note that the new measure dP_B is within the exponential family. An advantage of this is that we can easily manipulate the mean of $Z_B(t)$ under this new measure, which is $\dot{\psi}_B(\theta_B)$, by properly choosing θ_B . Specifically, we will choose θ_B such that $\dot{\psi}_B(\theta_B) = b$.

- (ii) We will apply likelihood ratio identity. Before this, we first define some terms: the log-likelihood ratio is

$$\ell_B(t) = \log(dP_B/d\mathbb{P}_\infty) = \theta_B Z_B(t) - \psi_B(\theta_B).$$

The *global term* is $\tilde{\ell}_B(t) = \theta_B (Z_B(t) - b)$ and *local terms* are

$$M_B = \max_{t \in [m], s \in [2:w]} e^{\ell_s(t) - \ell_B(t)},$$

$$S_B = \sum_{t=1}^m \sum_{s \in [2:w]} e^{\ell_s(t) - \ell_B(t)}.$$

For notational simplicity, we denote

$$\Omega = [m] \times [2 : w].$$

By likelihood ratio identity, $\mathbb{E}[X; A] = \mathbb{E}[X \mathbb{1}_A]$, where $\mathbb{1}_A = 1$ if event A is true and

zero otherwise, we have

$$\begin{aligned}
\mathbb{P}_\infty \left(\max_{(t,B) \in \Omega} Z_B(t) \geq b \right) &= \mathbb{E}_\infty \left[1; \max_{(t,B) \in \Omega} Z_B(t) \geq b \right] \\
&= \mathbb{E}_\infty \left[\underbrace{\frac{\sum_{(t,B) \in \Omega} e^{\ell_B(t)}}{\sum_{(t,s) \in \Omega} e^{\ell_s(t)}}}_{=1}; \max_{(t,B) \in \Omega} Z_B(t) \geq b \right] \\
&= \sum_{(t,B) \in \Omega} \mathbb{E}_\infty \left[\frac{e^{\ell_B(t)}}{\sum_{(t,s) \in \Omega} e^{\ell_s(t)}}; \max_{(t,B) \in \Omega} Z_B(t) \geq b \right] \\
&= \sum_{(t,B) \in \Omega} \mathbb{E}_B \left[\frac{1}{\sum_{(t,s) \in \Omega} e^{\ell_s(t)}}; \max_{(t,B) \in \Omega} Z_B(t) \geq b \right] \\
&= m \sum_{B=2}^w e^{\psi_B(\theta_B) - \theta_B b} \mathbb{E}_B \left[\frac{M_B}{S_B} e^{-(\tilde{\ell}_B + \log M_B)}; \tilde{\ell}_B + \log M_B \geq 0 \right].
\end{aligned}$$

(iii) We invoke localization theorem (see, e.g., [Siegmund et al. \[2010\]](#) and [Yakir \[2013\]](#), for details) to show the asymptotic independence of local fields and global term in the equation above. Matching the equation in step (ii) above to [\(24\)](#), we know that

$$\lambda = \sum_{B=2}^w e^{\psi_B(\theta_B) - \theta_B b} \mathbb{E}_B \left[\frac{M_B}{S_B} e^{-(\tilde{\ell}_B + \log M_B)}; \tilde{\ell}_B + \log M_B \geq 0 \right].$$

Therefore, the ARL can be approximated as $1/\lambda$. To evaluate the expectation in the above equation, we investigate the covariance structure of this random field as in [Lemma 4](#). As suggested by [Xie and Xie \[2021\]](#), we can just consider taking $B_1 = B_2 = B$ in [Lemma 4](#) when evaluating the covariance and doing this can still maintain the required level of accuracy. Therefore, the covariance structure is exactly the same with the one in [Li et al. \[2019\]](#) under the online setting, and the rest of the proof directly follows the proof therein. □

In addition to the proof of the ARL approximation, we also show how to further simplify the expression when we only consider the first two moments' information as follows:

Derivation of equation [\(12\)](#). As $\mu \rightarrow \infty$, we have

$$\nu(\mu) \approx \frac{(2/\mu)(\Phi(\mu/2) - 0.5)}{(\mu/2)\Phi(\mu/2) + \phi(\mu/2)} = \frac{2}{\mu^2}(1 + o(1)).$$

Therefore, by plugging (11) into (10), we have $\mathbb{E}_\infty[T_w]$ expressed as follows:

$$\begin{aligned}
& \frac{\sqrt{2\pi}}{b} \left\{ \sum_{B=2}^w e^{-b^2/2} \frac{(2B-1)}{B(B-1)} \frac{2}{\left(b\sqrt{\frac{2(2B-1)}{B(B-1)}}\right)^2} \right\}^{-1} \\
&= \frac{\sqrt{2\pi}}{b} e^{b^2/2} \left\{ \sum_{B=2}^w \frac{(2B-1)}{B(B-1)} \frac{B(B-1)}{b^2(2B-1)} \right\}^{-1} (1 + o(1)) \\
&= \frac{\sqrt{2\pi}b}{w} e^{b^2/2} (1 + o(1)).
\end{aligned}$$

C Proof of Lemma 3

In this subsection, we will formally prove Lemma 3. This proof involves many technical details, but the high level idea is simple. To help readers understand this simple idea, we first sketch this proof. For notational simplicity, we denote the detection statistic of our procedure as:

$$Z_t = \max_{B \in [2:w]} Z_B(t), \quad (26)$$

where $Z_B(t)$ is the Scan B -statistic defined in (3).

In the following, to improve readability, we first sketch the proof of Lemma 3 since it requires several technical lemmas. After that, we will prove all technical results rigorously.

Proof of Lemma 3. On one hand, for large enough window length choice (15), the detection procedure will not stop too early nor too late. To be precise, for any $w \geq 7b/(\rho\mathcal{D}(p, q))$ and $t_1 = b/(4\rho\mathcal{D}(p, q))$, as $b \rightarrow \infty$, we will have

$$\mathbb{P}_0(T_w < t_1) \leq 2t_1^2 \left(\exp \left\{ -\frac{Nb^2}{512K^2} \right\} + \exp \left\{ -\frac{b^2}{128K^2} \right\} \right), \quad (27)$$

$$\mathbb{P}_0(T_w > w) \leq \left(2 \exp \left\{ -\frac{Nb^2}{512K^2} \right\} + 2 \exp \left\{ -\frac{b^3}{128\rho\mathcal{D}(p, q)K^2} \right\} \right)^{\frac{4b}{\rho\mathcal{D}(p, q)}}. \quad (28)$$

On the other hand, for any $t \in [t_1, w]$, we can show that for our detection statistic $Z_t = \max_{B \in [2:w]} Z_B(t)$, the maximum is attained at $B = t$ with high probability. To be

precise, we denote $B_1(t) = t/(8(\rho\mathcal{D}(p, q) \vee 1))$, and

$$\begin{aligned} A_{1,t} &= \left\{ \max_{2 \leq B \leq t \wedge w} Z_B(t) = \max_{B_1(t) \leq B \leq t} Z_B(t) \right\}, \\ A_{2,t} &= \left\{ \max_{B_1(t) \leq B \leq t} Z_B(t) = Z_t(t) \right\}, \end{aligned} \quad (29)$$

For any $t \in [t_1, w]$, as $b \rightarrow \infty$, we will have

$$\begin{aligned} \mathbb{P}_0(A_{t,1}^c) &\leq \frac{b}{16(\rho\mathcal{D}^2(p, q) \vee 1)} \left(\exp \left\{ -\frac{Nb^2}{2^{15}(\rho\mathcal{D}^2(p, q) \vee 1)K^2} \right\} \right. \\ &\quad \left. + \exp \left\{ -\frac{b^2}{2^{13}(\rho\mathcal{D}^2(p, q) \vee 1)K^2} \right\} \right) (1 + o(1)), \end{aligned} \quad (30)$$

$$\mathbb{P}_0(A_{t,2}^c) \leq 6 \left(\exp \left\{ -\frac{b\rho\mathcal{D}(p, q)}{2^{13}(\rho\mathcal{D}(p, q) \vee 1)K^2} \right\} + \exp \left\{ -\frac{N\rho\mathcal{D}^2(p, q)}{512K^2} \right\} \right) (1 + o(1)), \quad (31)$$

where the superscript c denotes the complement of a set.

Now, equations (27) and (28) tell us T_w takes value from $[t_1, w]$ with high probability, and equations (30) and (31) show that at time $t \in [t_1, w]$, with high probability, the maximum over $B \in [2 : w]$ is attained at $B = t$. These enable us to calculate the expectation of detection statistic at the stopping time as follows:

$$\begin{aligned} \left| \mathbb{E}_0[Z_{T_w}] - \rho\mathcal{D}(p, q)\mathbb{E}_0[T_w] \right| &\leq \left(\rho\mathcal{D}(p, q) + 12K \exp \left\{ -\frac{N\rho\mathcal{D}^2(p, q)}{512K^2} \right\} \right. \\ &\quad \left. + 12K \exp \left\{ -\frac{b\rho\mathcal{D}(p, q)}{2^{13}(\rho\mathcal{D}(p, q) \vee 1)K^2} \right\} \right) (1 + o(1)). \end{aligned} \quad (32)$$

Finally, since the overshoot, which is the occurrence of detection statistic exceeding its target threshold b , will be $o(1)$ given that $b \rightarrow \infty$, we will have the detection statistic at $t = T_w$ approximated as follows:

$$\mathbb{E}_0[Z_{T_w}] = b(1 + o(1)). \quad (33)$$

By equations (32) and (33), we complete the proof. Detailed statement and proof of equations (27) and (28) can be found in Lemma 8. Equations (30) and (31) are proved in Lemma 9. Equation (32) is proved in Lemma 10. \square

Now, we will present and prove the technical lemmas used in the above proof sketch. We

will start with an important concentration result for the Scan B -statistic. Recall its definition in (3) as follows:

$$Z_B(t) = \frac{\sum_{i=1}^N \widehat{\mathcal{D}}(\mathbf{X}_B^{(i)}, \mathbf{Y}_B(t))}{N \sqrt{\text{Var}_\infty(\widehat{\mathcal{D}}_B(t))}}.$$

As we can see, the difficulty comes from that the average in Scan B -statistic is taken over correlated random variables since we reuse the post-change block $\mathbf{Y}_B(t)$. Nevertheless, we can leverage the Azuma's inequality for martingale and get the following concentration result for Scan B -statistic:

Lemma 7 (Concentration inequality for Scan B -statistic). For any window length choice $w \geq 2$, at time step $t \leq w$, for any block size $B_0 \in [2 : w]$, the Scan B -statistic $Z_{B_0}(t)$ (3) satisfies the following concentration inequality: for any $z_1, z_2 > 0$ and $z = z_1 + z_2$, we have

$$\mathbb{P}_0(|Z_{B_0}(t) - \mu_{B_0}(t)| \geq z) \leq 2 \exp\left\{-\frac{Nz_1^2}{32K^2}\right\} + 2 \exp\left\{-\frac{B_0z_2^2}{16K^2}\right\}, \quad (34)$$

where the expectation $\mu_{B_0}(t)$ has explicit formula as shown in Lemma 6.

Proof. For $z = z_1 + z_2 > 0$ (with $z_1, z_2 > 0$), event $\{|x - y| > z\}$ is a subset of event $\{|x - w| \geq z_1\} \cup \{|w - y| \geq z_2\}$, since if we take the complement we can easily show $\{|x - w| < z_1\} \cap \{|w - y| < z_2\} \subset \{|x - y| < z\}$. Let us define the following conditional expectation (which is a random variable),

$$f(\mathbf{Y}_B(t)) = \mathbb{E}_0 \left[\widehat{\mathcal{D}}(\mathbf{X}_B^{(1)}, \mathbf{Y}_B(t)) \mid \mathbf{Y}_B(t) \right].$$

We will have

$$\{|Z_{B_0}(t) - \mu_{B_0}(t)| \geq z\} \subset \{|Z_B(t) - f(\mathbf{Y}_B(t))| \geq z_1\} \cap \{|f(\mathbf{Y}_B(t)) - \mu_B(t)| \geq z_2\}. \quad (35)$$

On one hand, we can show

$$\sum_{i=1}^N \widehat{\mathcal{D}}(\mathbf{X}_B^{(i)}, \mathbf{Y}_B(t)) - Nf(\mathbf{Y}_B(t))$$

is a martingale with its difference bounded within $[-4K, 4K]$. Therefore, by Azuma's

inequality, for any $z > 0$, we have

$$\begin{aligned} \mathbb{P}_0(|Z_B(t) - f(\mathbf{Y}_B(t))| \geq z) &= \mathbb{P}_0\left(\left|\sum_{i=1}^N \widehat{\mathcal{D}}(\mathbf{X}_B^{(i)}, \mathbf{Y}_B(t)) - Nf(\mathbf{Y}_B(t))\right| \geq Nz\right) \\ &\leq 2 \exp\left\{-\frac{(Nz)^2}{32K^2N}\right\} = 2 \exp\left\{-\frac{Nz^2}{32K^2}\right\}. \end{aligned}$$

On the other hand, we can apply similar concentration inequality on the empirical estimator of MMD (with sample size B), which can be derived from the large deviation bound on U-statistics (cf. [Hoeffding \[1994\]](#) or Theorem 10 in [Gretton et al. \[2012a\]](#)). To be precise, for any $z > 0$, we have:

$$\mathbb{P}_0(|f(\mathbf{Y}_B(t)) - \mu_B(t)| \geq z) \leq 2 \exp\left\{-\frac{Bz^2}{16K^2}\right\}.$$

Finally, by [\(35\)](#) and the above two concentration inequalities, we can prove [\(34\)](#). \square

Lemma 8. Under H_1 where $p \neq q$, assume change occurs at time step 0, Under Assumptions [\(A1\)](#) and [\(A2\)](#), as $b \rightarrow \infty$, for any $N > 0$, we have:

(1) for any $t_1 < b/(2\rho\mathcal{D}(p, q))$, where constant ρ is defined in [\(14\)](#), the following holds for the stopping time of online kernel CUSUM T_w [\(8\)](#):

$$\mathbb{P}_0(T_w < t_1) \leq 2t_1^2 \left(\exp\left\{-\frac{Nb^2}{512K^2}\right\} + \exp\left\{-\frac{b^2}{128K^2}\right\} \right).$$

(2) for any $t_2 \geq 4b/(\rho\mathcal{D}(p, q))$, as long as we choose $w > 3b/(\rho\mathcal{D}(p, q))$, the following holds for T_w :

$$\begin{aligned} \mathbb{P}_0(T_w > t_2) &\leq \left(2 \exp\left\{-\frac{Nb^2}{512K^2}\right\} + 2 \exp\left\{-\frac{b^3}{128\rho\mathcal{D}(p, q)K^2}\right\} \right)^{t_2 - 3b/(\rho\mathcal{D}(p, q))} \\ &\leq \left(2 \exp\left\{-\frac{Nb^2}{512K^2}\right\} + 2 \exp\left\{-\frac{b^3}{128\rho\mathcal{D}(p, q)K^2}\right\} \right)^{b/(\rho\mathcal{D}(p, q))}. \end{aligned}$$

Proof. Let us prove (2) first. Intuitively, it is a rare event that T_w exceeds t_2 for such large

t_2 . By definition, we have:

$$\begin{aligned}\mathbb{P}_0(T_w > t_2) &= \mathbb{P}_0(\max_{2 \leq t \leq t_2} Z_t < b) = \prod_{t=2}^{t_2} \mathbb{P}_0(Z_t < b) \\ &= \prod_{t=2}^{t_2} \prod_{B=2}^{t \wedge w} \mathbb{P}_0(Z_B(t) < b).\end{aligned}$$

Here, due to our choice of t_2 , we have

$$\mathbb{P}_0(T_w > w) \leq \prod_{t=3b/(\rho\mathcal{D}(p,q))}^{t_2} \mathbb{P}_0(Z_{t \wedge w}(t) < b).$$

Notice that, as long as $B > 3b/(\rho\mathcal{D}(p,q)) > 4/3$, we have

$$\mathbb{E}_0[Z_B(t)] = \rho\mathcal{D}(p,q)\sqrt{B(B-1)} \geq \rho\mathcal{D}(p,q)\frac{B}{2} > \frac{3b}{2},$$

where the last inequality comes from the fact that $\sqrt{x(x-1)} > x/2, \forall x > 4/3$. The condition $3b/(\rho\mathcal{D}(p,q)) > 4/3$ can easily be satisfied as b goes to infinity. Finally, by Lemma 7, we have

$$\mathbb{P}_0(T_w > t_2) \leq \left(2 \exp \left\{ -\frac{Nb^2}{512K^2} \right\} + 2 \exp \left\{ -\frac{b^3}{128\rho\mathcal{D}(p,q)K^2} \right\} \right)^{t_2 - 3b/(\rho\mathcal{D}(p,q))}.$$

Next, let us prove (1). We have:

$$\begin{aligned}\mathbb{P}_0(T_w < t_1) &= \mathbb{P}_0(\max_{0 < t < t_1} Z_t \geq b) \\ &\leq \sum_{t=1}^{t_1} \mathbb{P}_0(Z_t \geq b) \leq \sum_{t=1}^{t_1} \sum_{B=2}^{t \wedge w} \mathbb{P}_0(Z_B(t) \geq b).\end{aligned}$$

Similarly, notice that

$$\mathbb{E}_0[Z_B(t)] = \rho\mathcal{D}(p,q)\sqrt{B(B-1)} \leq \rho\mathcal{D}(p,q)t_1 < b/2,$$

where the last inequality is guaranteed by the choice of t_1 . Again, by Lemma 7, we have

$$\begin{aligned}\mathbb{P}_0(T_w < t_1) &= \mathbb{P}_0\left(\max_{0 < t < t_1} Z_t \geq b\right) \leq \sum_{t=1}^{t_1} \mathbb{P}_0(Z_t \geq b) \leq \sum_{t=1}^{t_1} \sum_{B=2}^{t \wedge w} \mathbb{P}_0(Z_B(t) \geq b) \\ &\leq t_1^2 \left(2 \exp \left\{ -\frac{N(b/4)^2}{32K^2} \right\} + 2 \exp \left\{ -\frac{2(b/4)^2}{16K^2} \right\} \right).\end{aligned}$$

Now we complete the proof. □

Lemma 9. Under H_1 , where $p \neq q$ and we assume change occurs at time step 0, and Under Assumptions (A1) and (A2), we choose

$$t_1 = \frac{b}{4\rho\mathcal{D}(p, q)}, \quad w > \frac{3b}{\rho\mathcal{D}(p, q)},$$

which satisfies the constraints in Lemma 8 and constant ρ is defined in (14), we further take

$$B_1(t) = \frac{t}{8(\rho\mathcal{D}(p, q) \vee 1)},$$

for any $t \in [t_1, w]$, recall that we denote

$$\begin{aligned}A_{1,t} &= \left\{ \max_{2 \leq B \leq t \wedge w} Z_B(t) = \max_{B_1(t) \leq B \leq t} Z_B(t) \right\}, \\ A_{2,t} &= \left\{ \max_{B_1(t) \leq B \leq t} Z_B(t) = Z_t(t) \right\},\end{aligned}$$

for any $N > 0$, as long as $t_1 > 4/3$, the following holds

$$\begin{aligned}\mathbb{P}_0(A_{1,t}^c) &\leq 2 \left(\exp \left\{ -\frac{Nb^2}{2^{13}(\rho\mathcal{D}^2(p, q) \vee 1)K^2} \right\} + \exp \left\{ -\frac{(\rho\mathcal{D}^2(p, q) \wedge 1)b^3}{2^{14}\rho\mathcal{D}(p, q)^3K^2} \right\} \right) \\ &\quad + \frac{b}{16(\rho\mathcal{D}^2(p, q) \vee 1)} \exp \left\{ -\frac{Nb^2}{2^{15}(\rho\mathcal{D}^2(p, q) \vee 1)K^2} \right\} \\ &\quad + \frac{b}{16(\rho\mathcal{D}^2(p, q) \vee 1)} \exp \left\{ -\frac{b^2}{2^{13}(\rho\mathcal{D}^2(p, q) \vee 1)K^2} \right\}.\end{aligned}$$

Therefore, as $b \rightarrow \infty$, we have

$$\mathbb{P}_0(A_{t,1}^c) \leq \frac{b}{16(\rho\mathcal{D}^2(p,q) \vee 1)} \left(\exp \left\{ -\frac{Nb^2}{2^{15}(\rho\mathcal{D}^2(p,q) \vee 1)K^2} \right\} + \exp \left\{ -\frac{b^2}{2^{13}(\rho\mathcal{D}^2(p,q) \vee 1)K^2} \right\} \right) (1 + o(1)).$$

Similarly, as $b \rightarrow \infty$, we have

$$\mathbb{P}_0(A_{t,2}^c) \leq 6 \left(\exp \left\{ -\frac{N\rho\mathcal{D}^2(p,q)}{512K^2} \right\} + \exp \left\{ -\frac{b\rho\mathcal{D}(p,q)}{2^{13}(\rho\mathcal{D}(p,q) \vee 1)K^2} \right\} \right) (1 + o(1)).$$

Proof. Firstly, we will deal with $\mathbb{P}_0(A_{t,1}^c)$. We let

$$t_3 = (\rho\mathcal{D}(p,q) \wedge 1)t/4 \tag{36}$$

and denote

$$\tilde{A}_{1,t} = \left\{ \max_{B_1(t) \leq B \leq t} Z_B(t) > t_3 \right\}.$$

Then, we have

$$\mathbb{P}_0(\tilde{A}_{1,t}) \geq \mathbb{P}_0(Z_t(t) > t_3) = 1 - \mathbb{P}_0(Z_t(t) \leq t_3).$$

Notice that for any $t \geq t_1 > 4/3$, we have

$$\mathbb{E}_0[Z_t(t)] = \rho\mathcal{D}(p,q)\sqrt{t(t-1)} \geq \rho\mathcal{D}(p,q)\frac{t}{2} \geq 2t_3,$$

where the first inequality comes from the fact that $\sqrt{x(x-1)} > x/2$, $\forall x > 4/3$ and the second inequality comes from our choice of t_3 (36). Therefore, by Lemma 7, we have

$$\begin{aligned} \mathbb{P}_0(\tilde{A}_{1,t}^c) &\leq \mathbb{P}_0(Z_t(t) \leq t_3) \leq 2 \left(\exp \left\{ -\frac{Nt_3^2}{32K^2} \right\} + \exp \left\{ -\frac{t t_3^2}{16K^2} \right\} \right) \\ &\leq 2 \left(\exp \left\{ -\frac{N(\rho\mathcal{D}^2(p,q) \wedge 1)t^2}{512K^2} \right\} + \exp \left\{ -\frac{(\rho\mathcal{D}^2(p,q) \wedge 1)t^3}{256K^2} \right\} \right). \end{aligned} \tag{37}$$

Now, we have

$$\begin{aligned}
\mathbb{P}_0(A_{1,t}^c) &= \mathbb{P}_0(A_{1,t}^c \cap \tilde{A}_{1,t}^c) + \mathbb{P}_0(A_{1,t}^c \cap \tilde{A}_{1,t}) \\
&\leq \mathbb{P}_0(\tilde{A}_{1,t}^c) + \mathbb{P}_0(A_{1,t}^c \cap \tilde{A}_{1,t}) \\
&\leq \mathbb{P}_0(\tilde{A}_{1,t}^c) + \mathbb{P}_0\left(\max_{2 \leq B < B_1(t)} Z_B(t) > t_3\right) \\
&\leq \mathbb{P}_0(\tilde{A}_{1,t}^c) + \sum_{B=2}^{B_1(t)} \mathbb{P}_0(Z_B(t) > t_3).
\end{aligned}$$

Similarly, notice that $\mathbb{E}_0[Z_B(t)] \leq \rho\mathcal{D}(p, q)B_1(t) \leq t_3/2$, we have

$$\begin{aligned}
\sum_{B=2}^{B_1(t)} \mathbb{P}_0(Z_B(t) > t_3) &\leq 2B_1(t) \left(\exp\left\{-\frac{N(t_3/2)^2}{32K^2}\right\} + \exp\left\{-\frac{2(t_3/2)^2}{16K^2}\right\} \right) \\
&\leq \frac{t}{4(\rho\mathcal{D}(p, q) \vee 1)} \left(\exp\left\{-\frac{N(\rho\mathcal{D}^2(p, q) \wedge 1)t^2}{2048K^2}\right\} \right. \\
&\quad \left. + \exp\left\{-\frac{(\rho\mathcal{D}^2(p, q) \wedge 1)t^2}{512K^2}\right\} \right).
\end{aligned}$$

Notice that we already have bounded $\mathbb{P}_0(\tilde{A}_{1,t}^c)$ in (37). Here, we can observe that the rate of the above probability upper bound vanishing to zero depends on $t \in [t_1, w]$. The choice of t_1 in Lemma 8 only needs to satisfy $t_1 < b/(2\rho\mathcal{D}(p, q))$. Therefore, we will choose $t_1 = b/(4\rho\mathcal{D}(p, q))$ here. This gives us the desired upper bound on $\mathbb{P}_0(A_{1,t}^c)$.

Next, we handle event $A_{t,2}$. Recall that we denote the expectation of $Z_B(t)$ as $\mu_B(t)$, which is evaluated in Lemma 6. Denote $\delta_2 = \rho\mathcal{D}(p, q)/2$, and we have

$$\begin{aligned}
\mu_B(t) - \mu_{B-1}(t) &= \rho\mathcal{D}(p, q)(\sqrt{B(B-1)} - \sqrt{(B-1)(B-2)}) \\
&= \frac{2\sqrt{B-1}}{\sqrt{B} + \sqrt{B-2}} \rho\mathcal{D}(p, q) > \rho\mathcal{D}(p, q).
\end{aligned}$$

Here, the last inequality comes from the fact that $\frac{2\sqrt{B-1}}{\sqrt{B} + \sqrt{B-2}} > 1$, which can be verified by taking square and re-arranging terms. Now, by definition, we have

$$\{|Z_B(t) - \mu_B(t)| < \mu_t(t) - \mu_B(t) - \delta_2, B \in [B_1(t), t-1]\} \cap \{|Z_t(t) - \mu_t(t)| < \delta_2\} \subset A_{t,2}.$$

This gives us

$$\begin{aligned}\mathbb{P}_0(A_{t,2}^c) &\leq \sum_{B=B_1(t)}^{t-1} \mathbb{P}_0(|Z_B(t) - \mu_B(t)| < \mu_t(t) - \mu_B(t) - \delta_2) + \mathbb{P}_0(|Z_t(t) - \mu_t(t)| < \delta_2) \\ &\leq \sum_{B=B_1(t)}^{t-1} \mathbb{P}_0(|Z_B(t) - \mu_B(t)| < \delta_2(1 + 2(t-1-B))) + \mathbb{P}_0(|Z_t(t) - \mu_t(t)| < \delta_2).\end{aligned}$$

Notice that the last inequality comes from the following derivation: $\mu_t(t) - \mu_B(t) - \delta_2 = \mu_t(t) - \mu_{B+1}(t) + (\mu_{B+1}(t) - \mu_B(t) - \delta_2)$. As we have shown above, $\mu_{B+1}(t) - \mu_B(t) > \rho\mathcal{D}(p, q) = 2\delta_2$, therefore we have

$$\begin{aligned}\mu_t(t) - \mu_B(t) - \delta_2 &> \mu_t(t) - \mu_{B+1}(t) + \delta_2 \\ &= 2\delta_2(\sqrt{t(t-1)} - \sqrt{B(B+1)}) + \delta_2.\end{aligned}$$

What remains to be proved is $\sqrt{t(t-1)} - \sqrt{B(B+1)} > t-1-B$. Again, this can be verified by taking square and re-arranging terms. We omit further details for this simple derivation here. Now, by Lemma 7, we have

$$\begin{aligned}\mathbb{P}_0(A_{t,2}^c) &\leq 2 \sum_{B=B_1(t)}^{t-1} \left(\exp \left\{ -\frac{N[(t-B-1/2)\delta_2]^2}{32K^2} \right\} + \exp \left\{ -\frac{B[(t-B-1/2)\delta_2]^2}{16K^2} \right\} \right) \\ &\quad + 2 \exp \left\{ -\frac{N(\delta_2/2)^2}{32K^2} \right\} + 2 \exp \left\{ -\frac{t(\delta_2/2)^2}{16K^2} \right\} \\ &\leq 2 \sum_{B=B_1(t)}^{t-1} \left(\exp \left\{ -\frac{N[(t-B-1/2)\delta_2]^2}{32K^2} \right\} + \exp \left\{ -\frac{B_1(t)[(t-B-1/2)\delta_2]^2}{16K^2} \right\} \right) \\ &\quad + 2 \exp \left\{ -\frac{N(\delta_2/2)^2}{32K^2} \right\} + 2 \exp \left\{ -\frac{t(\delta_2/2)^2}{16K^2} \right\}.\end{aligned}$$

By the summation of geometric series, we can bound the above summation. We omit further details on the derivation.

We should remark that $B_1(t) = t/(8(\rho\mathcal{D}(p, q) \vee 1)) \geq t_1/(8(\rho\mathcal{D}(p, q) \vee 1))$ can not be overly small. That is to say, we cannot choose overly small t_1 in Lemma 8, which happens to agree with what we have done for event $A_{t,1}$ above. Here, the reason is that the concentration of Scan B -statistic depends on not only the number of blocks N , but also the block size B , which is lower bounded by $B_1(t)$ in the above analysis. The above choice $t_1 = b/(4\rho\mathcal{D}(p, q))$

suffices to give a good enough rate of concentration. Now, as $N \rightarrow \infty$ and $b \rightarrow \infty$, we have

$$\mathbb{P}_0(A_{t,2}^c) \leq 6 \left(\exp \left\{ -\frac{N\delta_2^2}{128K^2} \right\} + \exp \left\{ -\frac{B_1(t)\delta_2^2}{64K^2} \right\} \right) (1 + o(1)).$$

Moreover, by our choice $t_1 = b/(4\rho\mathcal{D}(p, q))$, we can further bound the above term for all $t \in [t_1, w]$ as follows:

$$\mathbb{P}_0(A_{t,2}^c) \leq 6 \left(\exp \left\{ -\frac{N\rho\mathcal{D}^2(p, q)}{512K^2} \right\} + \exp \left\{ -\frac{b\rho\mathcal{D}(p, q)}{2^{13}(\rho\mathcal{D}(p, q) \vee 1)K^2} \right\} \right) (1 + o(1)).$$

We complete the proof. □

Lemma 10. Under H_1 , where $p \neq q$ and we assume change occurs at time step 0, and Under Assumptions (A1) and (A2), we choose

$$w \geq \frac{7b}{\rho\mathcal{D}(p, q)},$$

where constant ρ is defined in (14), as $b \rightarrow \infty$, for any $N > 0$, we have

$$\begin{aligned} |\mathbb{E}_0[Z_{T_w}] - \rho\mathcal{D}(p, q)\mathbb{E}_0[T_w]| &\leq \left(\rho\mathcal{D}(p, q) + 12K \exp \left\{ -\frac{N\rho\mathcal{D}^2(p, q)}{512K^2} \right\} \right. \\ &\quad \left. + 12K \exp \left\{ -\frac{b\rho\mathcal{D}(p, q)}{2^{13}(\rho\mathcal{D}(p, q) \vee 1)K^2} \right\} \right) (1 + o(1)). \end{aligned}$$

Proof. Step 1: We choose $w = 4b/(\rho\mathcal{D}(p, q))$ as in Lemma 9. For any $t \in [t_1, w]$, recall the

definitions of events $A_{1,t}$ and $A_{2,t}$ in (29), we will have

$$\begin{aligned}
\mathbb{E}_0 \left[\max_{2 \leq B \leq B_{\max}} Z_B(t) \right] &= \mathbb{E}_0 \left[\max_{B_1 \leq B \leq B_2} Z_B(t); A_1 \right] + \mathbb{E}_0 \left[\max_{2 \leq B \leq B_{\max}} Z_B(t); A_1^c \right] \\
&= \mathbb{E}_0 \left[\max_{B_1 \leq B \leq B_2} Z_B(t) \right] + \mathbb{E}_0 \left[\max_{2 \leq B \leq B_{\max}} Z_B(t); A_1^c \right] \\
&= \mathbb{E}_0 \left[\max_{B_1 \leq B \leq B_2} Z_B(t) - Z_t(t) \right] + \mathbb{E}_0 [Z_t(t)] + \mathbb{E}_0 \left[\max_{2 \leq B \leq B_{\max}} Z_B(t); A_1^c \right] \\
&= \rho \mathcal{D}(p, q) \sqrt{t(t-1)} \\
&\quad + \mathbb{E}_0 \left[\max_{B_1 \leq B \leq B_2} Z_B(t) - Z_t(t); A_2^c \right] + \mathbb{E}_0 \left[\max_{2 \leq B \leq B_{\max}} Z_B(t); A_1^c \right] \\
&= \rho \mathcal{D}(p, q) t + \rho \mathcal{D}(p, q) (\sqrt{t(t-1)} - t) \\
&\quad + \mathbb{E}_0 \left[\max_{B_1 \leq B \leq B_2} Z_B(t) - Z_t(t); A_2^c \right] + \mathbb{E}_0 \left[\max_{2 \leq B \leq B_{\max}} Z_B(t); A_1^c \right].
\end{aligned}$$

As we have shown in Lemma 9, we can easily bound $\mathbb{P}_0(A_1^c), \mathbb{P}_0(A_2^c)$. We have, $\forall t \in [t_1, w]$,

$$\left| \mathbb{E}_0 \left[\max_{B \in [2:w]} Z_B(t) \right] - \rho \mathcal{D}(p, q) t \right| \leq \rho \mathcal{D}(p, q) + 2K(\mathbb{P}_0(A_1^c) + \mathbb{P}_0(A_2^c)). \quad (38)$$

Step 2: We are ready to evaluate $\mathbb{E}_0[Z_{T_w}]$. Notice that $-2K \leq Z_B(t) \leq 2K$, the partition theorem gives us

$$\begin{aligned}
\mathbb{E}_0[Z_{T_w}] &= \mathbb{E}_0[Z_{T_w} | T_w < t_1] \mathbb{P}_0(T_w < t_1) \\
&\quad + \mathbb{E}_0[Z_{T_w} | T_w > w] \mathbb{P}_0(T_w > w) \\
&\quad + \mathbb{E}_0[Z_{T_w} | t_1 \leq T_w \leq w] \mathbb{P}_0(t_1 \leq T_w \leq w).
\end{aligned}$$

Combining everything above, we have

$$\begin{aligned}
|\mathbb{E}_0[Z_{T_w}] - \mathbb{E}_0[Z_{T_w} | t_1 \leq T_w \leq w]| &\leq 2K(\mathbb{P}_0(T_w > w) + \mathbb{P}_0(T_w < t_1) + 1 - \mathbb{P}_0(t_1 \leq T_w \leq w)) \\
&= 4K(\mathbb{P}_0(T_w > w) + \mathbb{P}_0(T_w < t_1)).
\end{aligned}$$

Recall that in Lemma 8, we have bounded both probabilities.

In the above equation, $\mathbb{E}_0[Z_{T_w} | t_1 \leq T_w \leq w]$ can be evaluated by replacing t with $[T_w | t_1 \leq T_w \leq w]$ and taking expectation with respect to $[T_w | t_1 \leq T_w \leq w]$. Combing

everything gives us

$$\begin{aligned} & |\mathbb{E}_0[Z_{T_w}] - \rho\mathcal{D}(p, q)\mathbb{E}_0[T_w | t_1 \leq T_w \leq w]| \\ & \leq \rho\mathcal{D}(p, q) + 2K\mathbb{P}_0(A_1^c) + 2K\mathbb{P}_0(A_2^c) + 4K\mathbb{P}_0(T_w > w) + 4K\mathbb{P}_0(T_w < t_1). \end{aligned}$$

Step 3: Now, we only need to bound the difference between $\mathbb{E}_0[T_w | t_1 \leq T_w \leq w]$ and $\mathbb{E}_0[T_w]$. Again, we apply partition theorem and will get

$$\begin{aligned} \mathbb{E}_0[T_w] &= \mathbb{E}_0[T_w | T_w < t_1]\mathbb{P}_0(T_w < t_1) \\ &+ \mathbb{E}_0[T_w | T_w > w]\mathbb{P}_0(T_w > w) \\ &+ \mathbb{E}_0[T_w | t_1 \leq T_w \leq w]\mathbb{P}_0(t_1 \leq T_w \leq w). \end{aligned}$$

On one hand, it is easy to show that

$$0 \leq \mathbb{E}_0[T_w | T_w < t_1]\mathbb{P}_0(T_w < t_1) \leq t_1\mathbb{P}_0(T_w < t_1).$$

On the other hand, we have

$$0 \leq \mathbb{E}_0[T_w | T_w > w] = \sum_{\tau=w}^{\infty} \mathbb{P}_0(T_w > \tau) + w\mathbb{P}_0(T_w > w).$$

Here, for $\tau \geq w = 4b/\rho\mathcal{D}(p, q)$, Lemma 8 and its proof therein give us

$$\mathbb{P}_0(T_w > \tau) \leq \left(2 \exp \left\{ -\frac{Nb^2}{512K^2} \right\} + 2 \exp \left\{ -\frac{b^3}{128\rho\mathcal{D}(p, q)K^2} \right\} \right)^{\tau-3b/(\rho\mathcal{D}(p, q))}.$$

Therefore, we have

$$\sum_{\tau=w}^{\infty} \mathbb{P}_0(T_w > \tau) \leq \frac{\left(2 \exp \left\{ -\frac{Nb^2}{512K^2} \right\} + 2 \exp \left\{ -\frac{b^3}{128\rho\mathcal{D}(p, q)K^2} \right\} \right)^{w-3b/(\rho\mathcal{D}(p, q))}}{1 - \left(2 \exp \left\{ -\frac{Nb^2}{512K^2} \right\} + 2 \exp \left\{ -\frac{b^3}{128\rho\mathcal{D}(p, q)K^2} \right\} \right)}.$$

Under the technical condition

$$b \geq (4\rho\mathcal{D}(p, q)/9 \vee 32\sqrt{2\log 2K}), \tag{39}$$

we are able to show

$$\begin{aligned} 2 \exp \left\{ -\frac{Nb^2}{512K^2} \right\} + 2 \exp \left\{ -\frac{b^3}{128\rho\mathcal{D}(p,q)K^2} \right\} &\leq 4 \exp \left\{ -\frac{b^2}{128K^2} \left(\frac{N}{4} \wedge \frac{b}{\rho\mathcal{D}(p,q)} \right) \right\} \\ &\leq \exp \left\{ -\frac{b^2}{256K^2} \left(\frac{N}{4} \wedge \frac{b}{\rho\mathcal{D}(p,q)} \right) \right\} < 1/2. \end{aligned}$$

Thus, we have

$$\sum_{\tau=w}^{\infty} \mathbb{P}_0(T_w > \tau) \leq 2 \exp \left\{ -\frac{b^2}{256K^2} \left(\frac{N}{4} \wedge \frac{b}{\rho\mathcal{D}(p,q)} \right) (w - 3b/(\rho\mathcal{D}(p,q))) \right\}.$$

As $b \rightarrow \infty$, the technical condition (39) automatically holds (since we choose $w \geq 7b/(\rho\mathcal{D}(p,q))$).

Therefore, we have

$$\begin{aligned} w\mathbb{P}_0(T_w > w) + \sum_{\tau=w}^{\infty} \mathbb{P}_0(T_w > \tau) &\leq w \exp \left\{ -\frac{b^2}{256K^2} \left(\frac{N}{4} \wedge \frac{b}{\rho\mathcal{D}(p,q)} \right) (w - 3b/(\rho\mathcal{D}(p,q))) \right\} \\ &\quad + 2 \exp \left\{ -\frac{b^2}{128K^2} \left(\frac{N}{4} \wedge \frac{b}{\rho\mathcal{D}(p,q)} \right) (w - 3b/(\rho\mathcal{D}(p,q))) \right\}. \end{aligned} \tag{40}$$

We notice that for any $a_1, a_2 > 0$ and $a_1 - a_2 \geq \log 2$, we will have

$$xe^{-a_1x} < e^{-a_2x}, \quad \forall x > 1,$$

since $x < e^{(a_1-a_2)x} \leq e^{x \log 2} = 2^x$. Under the technical condition (39), we have

$$\frac{1}{2} \frac{b^2}{256K^2} \left(\frac{N}{4} \wedge \frac{b}{\rho\mathcal{D}(p,q)} \right) \geq \frac{1}{2} \frac{32^2 \times 2 \times \log 2 K^2}{256K^2} \frac{1}{4} = \log 2.$$

That is to say, for $w > 1$ (which holds for large enough b and our choice $w \geq 7b/(\rho\mathcal{D}(p,q))$),

we will have

$$\begin{aligned}
0 &\leq w\mathbb{P}_0(T_w > w) + \sum_{\tau=w}^{\infty} \mathbb{P}_0(T_w > \tau) \\
&\leq \exp\left\{-\frac{b^2}{512K^2}\left(\frac{N}{4} \wedge \frac{b}{\rho\mathcal{D}(p,q)}\right)(w - 6b/(\rho\mathcal{D}(p,q)))\right\} \\
&\quad + 2 \exp\left\{-\frac{b^2}{128K^2}\left(\frac{N}{4} \wedge \frac{b}{\rho\mathcal{D}(p,q)}\right)(w - 3b/(\rho\mathcal{D}(p,q)))\right\} \\
&\leq 3 \exp\left\{-\frac{b^2}{512K^2}\left(\frac{N}{4} \wedge \frac{b}{\rho\mathcal{D}(p,q)}\right)(w - 6b/(\rho\mathcal{D}(p,q)))\right\}. \\
&\leq 3 \exp\left\{-\frac{b^3}{512\rho\mathcal{D}(p,q)K^2}\left(\frac{N}{4} \wedge \frac{b}{\rho\mathcal{D}(p,q)}\right)\right\},
\end{aligned}$$

where the last inequality comes from our choice $w \geq 7b/(\rho\mathcal{D}(p,q))$.

Step 4: Finally, combining the above derivations, we have

$$\begin{aligned}
&|\mathbb{E}_0[T_w] - \mathbb{E}_0[T_w | t_1 \leq T_w \leq w]| \\
&\leq t_1\mathbb{P}_0(T_w < t_1) + w(1 - \mathbb{P}_0(t_1 \leq T_w \leq w)) + \mathbb{E}_0[T_w | T_w > w]\mathbb{P}_0(T_w > w).
\end{aligned}$$

This gives us

$$\begin{aligned}
|\mathbb{E}_0[Z_{T_w}] - \rho\mathcal{D}(p,q)\mathbb{E}_0[T_w]| &\leq 2K(\mathbb{P}_0(A_1^c) + \mathbb{P}_0(A_2^c)) + 4K(\mathbb{P}_0(T_w > w) + \mathbb{P}_0(T_w < t_1)) \\
&\quad + \rho\mathcal{D}(p,q)\left(1 + t_1\mathbb{P}_0(T_w < t_1) + w(1 - \mathbb{P}_0(t_1 \leq T_w \leq w))\right. \\
&\quad \left.+ \mathbb{E}_0[T_w | T_w > w]\mathbb{P}_0(T_w > w)\right).
\end{aligned}$$

As $b \rightarrow \infty$, we only consider the leading term and will get

$$\begin{aligned}
|\mathbb{E}_0[Z_{T_w}] - \rho\mathcal{D}(p,q)\mathbb{E}_0[T_w]| &\leq \left(\rho\mathcal{D}(p,q) + 12K \exp\left\{-\frac{N\rho\mathcal{D}^2(p,q)}{512K^2}\right\}\right. \\
&\quad \left.+ 12K \exp\left\{-\frac{b\rho\mathcal{D}(p,q)}{2^{13}(\rho\mathcal{D}(p,q) \vee 1)K^2}\right\}\right)(1 + o(1)).
\end{aligned}$$

Now, we complete the proof. □

D Proof of Theorem 1

For notational simplicity, let us denote the detection statistic in the oracle detection procedure as follows:

$$Z_t^\circ = \max_{B \in [2:t]} Z_B(t), \quad (41)$$

where $Z_B(t)$ is the Scan B -statistic defined in (3).

Proof. It is important to recognize that we need to specify the choice of window length w when we control ARL by properly choosing threshold b . Thus the question boils down to the ARL approximation for given b and w . We will first show that it requires $w \sim b$ to guarantee ε -performance loss and therefore we need to show how to control ARL given the relationship $w \sim b$. Luckily, we can verify that the ARL approximation in Lemma 2 allows the window length w to go to infinity at any polynomial rate with respect to b (which includes the case $w \sim b$). To begin with, we prove that we need $w \sim b$ when there is a change at time zero to meet the ε -performance loss constraint.

Under H_1 . We assume change occurs at time step 0. Notice that the difference between our procedure and the oracle procedure only exists when $T_w > w$, otherwise, at time $t \leq w$, the scan region of our procedure would be $B \in [2 : w \wedge t]$, which is exactly the same with that of the oracle procedure. That is, we can upper bound the performance loss as follows:

$$\begin{aligned} 0 \leq \mathbb{E}_0[T_w] - \mathbb{E}_0[T_o] &\leq \mathbb{E}_0[T_w | T_w > w] \mathbb{P}_0(T_w > w) \\ &= w \mathbb{P}_0(T_w > w) + \sum_{\tau=w}^{\infty} \mathbb{P}_0(T_w > \tau). \end{aligned}$$

We re-use the derivations to bound $w \mathbb{P}_0(T_w > w)$ and $\sum_{\tau=w}^{\infty} \mathbb{P}_0(T_w > \tau)$ in the *step 3* in the proof of Lemma 10. Notice that, as $\gamma \rightarrow \infty$, by choosing $b \sim \log \gamma$, the technical conditions in that proof hold automatically. Thus, we have

$$\begin{aligned} 0 \leq \mathbb{E}_0[T_w] - \mathbb{E}_0[T_o] &\leq \exp \left\{ -\frac{b^2}{512K^2} \left(\frac{N}{4} \wedge \frac{b}{\rho \mathcal{D}(p, q)} \right) \left(w - \frac{6b}{\rho \mathcal{D}(p, q)} \right) \right\} \\ &\quad + 2 \exp \left\{ -\frac{b^2}{128K^2} \left(\frac{N}{4} \wedge \frac{b}{\rho \mathcal{D}(p, q)} \right) \left(w - \frac{3b}{\rho \mathcal{D}(p, q)} \right) \right\} \\ &\leq 3 \exp \left\{ -\frac{b^2}{512K^2} \left(\frac{N}{4} \wedge \frac{b}{\rho \mathcal{D}(p, q)} \right) \left(w - \frac{6b}{\rho \mathcal{D}(p, q)} \right) \right\}. \quad (42) \end{aligned}$$

Therefore, for any tolerance $\varepsilon > 0$, we only need the RHS of above inequality to be smaller

than ε . The sufficient condition to guarantee ε -performance loss is

$$w \geq \frac{6b}{\rho\mathcal{D}(p, q)} + \frac{512K^2 \log 3/\varepsilon}{b^2(N/4 \wedge b/(\rho\mathcal{D}(p, q)))}.$$

However, as we just mentioned, this is just a sufficient condition, meaning that the RHS of the above equation is just an upper bound of the smallest possible window length, i.e., w^* . We denote it by \bar{w} , i.e.,

$$\bar{w} = \frac{6b}{\rho\mathcal{D}(p, q)} + \frac{512K^2 \log 3/\varepsilon}{b^2(N/4 \wedge b/(\rho\mathcal{D}(p, q)))}.$$

Now we know that $w^* \leq \bar{w}$. Clearly, this \bar{w} is not exactly w^* since: (I) we manually choose $w > 3b/(\rho\mathcal{D}(p, q))$ to help bound $\mathbb{P}_0(T_w > w)$ in Lemma 8 and (II) the performance loss bound of $\mathbb{E}_0[T_w] - \mathbb{E}_0[T_o]$ in (42) is just an upper bound of the original performance loss bound in (40).

Nevertheless, we will show $w^* \sim \bar{w}$, meaning that we characterize the optimal memory efficient window length up to some constant factor. We will handle (II) first by showing that upper bound is tight in the sense that the resulting w to satisfy the ε -performance loss remains unchanged. Notice that we have already manually choose w to be $\mathcal{O}(b)$, by the upper bound on the performance loss bound (40), we have

$$\begin{aligned} & w\mathbb{P}_0(T_w > w) + \sum_{\tau=w}^{\infty} \mathbb{P}_0(T_w > \tau) \\ & \leq w \exp \left\{ -\frac{b^2}{256K^2} \left(\frac{N}{4} \wedge \frac{b}{\rho\mathcal{D}(p, q)} \right) (w - 3b/(\rho\mathcal{D}(p, q))) \right\} (1 + o(1)). \end{aligned}$$

For notational simplicity, we denote

$$\tilde{b} = \frac{b^2}{256K^2} \left(\frac{N}{4} \wedge \frac{b}{\rho\mathcal{D}(p, q)} \right).$$

Then, by the derivation in the *step 3* in the proof of Lemma 10, we have

$$\begin{aligned} \exp \left\{ -\tilde{b}(w - 3b/(\rho\mathcal{D}(p, q))) \right\} & \leq w \exp \left\{ -\tilde{b}(w - 3b/(\rho\mathcal{D}(p, q))) \right\} \\ & \leq \exp \left\{ -\frac{\tilde{b}}{2}(w - 6b/(\rho\mathcal{D}(p, q))) \right\}. \end{aligned}$$

As one can see, if we want LHS to meet the ε -performance loss constraint, the resulting

window length w will have the same order as \bar{w} , meaning that our performance bound is tight in terms of the order of the resulting window length to meet the ε -performance loss constraint.

Next, we handle (I). We will show choosing $w = o(b)$ cannot guarantee ε -performance loss for any fixed $\varepsilon > 0$, given $b \rightarrow \infty$. We need go back to the proof of Lemma 8 where we bound the probability $\mathbb{P}_0(T_w > w)$. Now, we choose $w = o(b)$ and will have

$$\mathbb{P}_0(T_w > w) = \mathbb{P}_0\left(\max_{t \in [2:w]} Z_t < b\right) = \prod_{t=2}^w \mathbb{P}_0(Z_t < b) = \prod_{t=2}^w \prod_{B=2}^{t \wedge w} \mathbb{P}_0(Z_B(t) < b).$$

Notice that, in Lemma 6, we calculated the expectation of the detection statistic, which is of order block size B . That is to say, for $B \leq w = o(b)$, we have

$$\begin{aligned} \mathbb{P}_0(Z_B(t) < b) &= 1 - \mathbb{P}_0(Z_B(t) \geq b) \\ &\geq 1 - 2 \exp\left\{-\frac{N(b-B)^2}{128K^2}\right\} - 2 \exp\left\{-\frac{B(b-B)^2}{64K^2}\right\} \\ &\geq 1 - 2 \exp\left\{-\frac{N(b-w)^2}{128K^2}\right\} - 2 \exp\left\{-\frac{2(b-w)^2}{64K^2}\right\}. \end{aligned}$$

Therefore, we have

$$\mathbb{P}_0(T_w > w) \geq \left(1 - 2 \exp\left\{-\frac{N(b-w)^2}{128K^2}\right\} - 2 \exp\left\{-\frac{2(b-w)^2}{64K^2}\right\}\right)^{w^2}.$$

Notice that $(1 - o(1/n))^n \rightarrow 1$ as $n \rightarrow \infty$. Clearly, as $b \rightarrow \infty$, for $w = o(b)$ choice, we have

$$2 \exp\left\{-\frac{N(b-w)^2}{128K^2}\right\} + 2 \exp\left\{-\frac{2(b-w)^2}{64K^2}\right\} = o(1/w^2).$$

That is to say, $\mathbb{P}_0(T_w > w) \rightarrow 1$ as $b \rightarrow \infty$. Recall that the performance loss bound has leading term $w\mathbb{P}_0(T_w > w)$, which cannot shrink to zero (or even diverge) as $b \rightarrow \infty$. Thus, $w = o(b)$ can never satisfy the ε -performance loss constraint and therefore our upper bound $w^* \leq \bar{w}$ is tight in terms of order.

Under H_0 . We choose detection threshold b to control the ARL, given that we choose $w \sim b$. The analytic approximation in Lemma 2 can partially answer the question — we are able to give the relationship between b and ARL to make sure our procedure is a constant ARL procedure in \mathcal{C}_γ (18). Luckily, our choice $w \sim b$ satisfies the technical condition in (23) and therefore we can apply this ARL approximation here. Even though it is difficult to obtain

such closed-form ARL approximation for the oracle procedure, we are able to leverage the concentration results for Scan B -statistic (Lemma 7 in Appendix C) to show it is also a constant ARL procedure in \mathcal{C}_γ .

For a given ARL, in our window-limited procedure (8), we approximate the true ARL $\mathbb{E}_\infty[T_w]$ using Lemma 2. The given ARL constraint is

$$\mathbb{E}_\infty[T_w] \geq \gamma. \quad (43)$$

For simplicity, we start with the coarse approximation under Gaussian assumption (i.e., we only use the first and the second order moments' information). By (12) as well as $w \sim b$, we have:

$$\mathbb{E}_\infty[T_w] \sim e^{b^2/2}. \quad (44)$$

To satisfy condition (43), we need

$$b = a\sqrt{\log \gamma}, \quad a \geq \sqrt{2}. \quad (45)$$

In follow-up discussion of Theorem 4.2 [Li et al., 2019], they explicitly claimed $\mathbb{E}_\infty[T_w] = \mathcal{O}(e^{b^2})$ and proposed to consider $b = \mathcal{O}(\sqrt{\log \gamma})$ in order to meet the ARL constraint (43), which agree with (44) and (45), respectively. However, we may notice that $b = \mathcal{O}(\sqrt{\log \gamma})$ might violate the lower bound in Lorden [1971], which is known as the best achievable EDD. Recall that the KL divergence is a fundamental information theoretic quantity which characterizes the hardness of the hypothesis testing problem. The Lorden's lower bound of EDD is on the order of $\log \gamma$ divided by the KL divergence, which will be larger than what we get above asymptotically since the KL divergence is treated as constant in our setting. This contradiction comes from the very coarse ARL approximation (see Figure 3), and if we incorporate the first $2n$ -th order moments' information in the ARL approximation (Lemma 2), we will have

$$\psi_B(\theta) \approx \sum_{i=1}^{2n} \frac{\mathbb{E}_\infty[Z_B^i(t)]}{i!} \theta^i.$$

Note that solving $\dot{\psi}_B(\theta_B) = b$ analytically is very challenging, but we can fix n and obtain

$$\theta_B \sim b^{1/(2n-1)},$$

when we consider the $b \rightarrow \infty$ limit, given that the $2n$ -th moment of the Scan B -statistic will

exist and not vanish to zero (Assumption (A1)). Plugging this into Lemma 2 gives us

$$\mathbb{E}_\infty[T_w] \sim \frac{e^{b^{2n/(2n-1)}}}{b^{\frac{4n-4}{2n-1}}}. \quad (46)$$

This yields a more strict condition on the threshold to be the ARL constraint (43), i.e.,

$$b \sim (\log \gamma)^{1-\frac{1}{2n}}. \quad (47)$$

We should remark that this is also numerically verified by Figure 3 in our experiment — considering higher order moment will lead to better approximation whereas fail to do so will result in “underestimating” threshold b . As one can see, the choice of detection threshold in (45) and will not satisfy the above requirement (47). Indeed, (45) corresponds to $n = 1$ case in (45). Thus, the threshold choice (45) will fail to meet the given ARL constraint asymptotically.

Now, both the numerical evidence and our theoretical analysis point out that the ARL approximation should involve all moments’ information to meet the given ARL constraint. In addition, recall that we also want to obtain the smallest possible window length w , which is on the same order with detection threshold b by our previous analysis. Thus, we give the optimal order of b as follows:

$$b \sim \log \gamma.$$

Although our current analysis cannot verify the conjecture that $\mathbb{E}_\infty[T_w] = \mathcal{O}(e^{c_3 b})$ for some constant $c_3 > 0$, (46) can tell us as $b \rightarrow \infty$

$$e^{c_3 b} / \mathbb{E}_\infty[T_w] \rightarrow 0.$$

This tells us that our procedure will keep running for a very long time when there is no change, and the run length will be much larger than the detection threshold b . At time step $t > w$, we will have

$$\max_{2 \leq B \leq t} Z_B(t) = Z_t^o \geq Z_t = \max_{2 \leq B \leq w} Z_B(t).$$

This implies the oracle procedure will stop earlier since it has larger detection statistics (for the same detection threshold). Here, approximating the ARL for the oracle procedure is not trivial and therefore the detection threshold for both procedures is selected based on

Lemma 2. By the above analysis, for b selected as

$$b \sim \log \gamma,$$

we know that

$$\begin{aligned} \mathbb{E}_\infty[T_w] &\geq \gamma, \\ \mathbb{E}_\infty[T_w] &\geq \mathbb{E}_\infty[T_o]. \end{aligned}$$

In the following, we will show $\mathbb{E}_\infty[T_o] \geq \gamma$. By our concentration result in Lemma 7, we have

$$\begin{aligned} \mathbb{P}_\infty(T_o \leq t_0) &= \mathbb{P}_\infty(\max_{1 \leq t \leq t_0} Z_t^o > b) = \mathbb{P}_\infty(\max_{1 \leq t \leq t_0} \max_{2 \leq B \leq t} Z_B(t) > b) \\ &= \mathbb{P}_\infty(\cup_{1 \leq t \leq t_0} \cup_{2 \leq B \leq t} \{Z_B(t) > b\}) \\ &\leq \sum_{1 \leq t \leq t_0} \sum_{2 \leq B \leq t} \mathbb{P}_\infty(Z_B(t) > b) = \mathcal{O}\left(t_0^2 \exp\left\{-\frac{2(b/2)^2}{16K^2}\right\}\right). \end{aligned}$$

This gives us $\mathbb{P}_\infty(T_o \leq \gamma)$ drops exponentially fast to zero with increasing b . That is to say, with probability almost one, the oracle procedure will not stop before $t_0 = \mathcal{O}(\gamma)$, which implies $\mathbb{E}_\infty[T_o] \geq \gamma$. Now, we complete the proof. □

E Additional Experimental Results

In this last section, we present additional experimental configurations and results. To begin with, we will use numerical evidence to guide users to select the detection procedure hyperparameters.

E.1 Study on the Hyperparameter Choices

In this part, we will study how the choices of the hyperparameters of our detection procedure influence the EDD. As mentioned above, the choice of window length w is very important and we will begin our numerical study with its effect on the EDD.

Recall that we use $[2 : w]$ as the search region to locate the change-point. Here, in addition to right end-point w , i.e., window length, we also study the effect of left end-point. Here, we use $[B_{\min} : B_{\max}]$ as the region in which we optimize block size parameter B ; we use w and B_{\max} interchangeably to denote the window length parameter. Intuitively, the wider

this search region is, the quicker the detection should be, but this merit comes with higher computational and memory costs. We validate this by comparing EDDs for a given ARL under different B_{\min} and B_{\max} choices and plot the results in Figure 9.

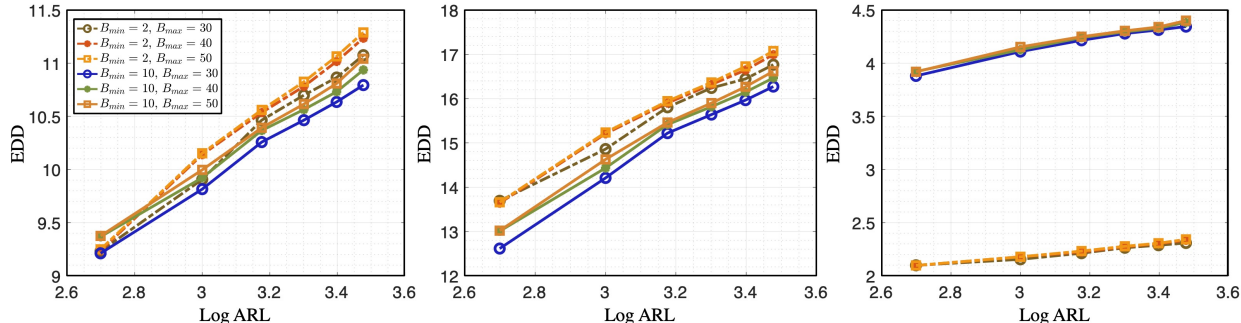


Figure 9: Comparison of EDD for different search regions $[B_{\min} : B_{\max}]$. The setting is: the pre-change distribution is $\mathcal{N}(\mathbf{0}_{20}, I_{20})$, and the post-change distributions are, from left to right, (a) $\mathcal{N}(\mathbf{0}_{20}, 0.01 I_{20})$; (b) $\mathcal{N}(\mathbf{0}_{20}, 0.2 I_{20})$; (c) $\mathcal{N}(\mathbf{0}_{20}, 9 I_{20})$.

From Figure 9, we observe that, on one hand, B_{\max} *controls the success of detection* — the detection procedure typically fails to raise an alarm within a reasonable time if EDD of the oracle procedure (41) exceeds B_{\max} . However, this does not tell users to choose an overly large window length, since (i) there is a trade-off between the EDD and the computational and memory cost and (ii) EDD improvement by choosing a larger window length w for a given ARL is no longer significant after $w \sim \log \text{ARL}$, as shown by our non-asymptotic study of the performance loss in Section 4.4. Most importantly, (ii) can be numerically verified by the leftmost panel in Figure 9 — As we can see, for $B_{\min} = 2$ case, the improvement of B_{\max} increasing from 40 to 50 is smaller than that of B_{\max} increasing from 30 to 40. In addition, in the rightmost panel, we can see the improvement of EDD by increasing B_{\max} is marginal. On the other hand, B_{\min} *is important to guarantee quick detection* — “power loss” will occur if B_{\min} is greater than EDD of the optimal procedure (41); see $B_{\min} = 10$ case in the rightmost panel for evidence. Otherwise, the effect of B_{\min} is negligible when the change is subtle. Here, a simple and safe choice would be $B_{\min} = 2$.

Next, we study the effect of kernel bandwidth on the EDD. As mentioned in Ramdas et al. [2015], the median heuristic gives the largest possible MMD (see observation 2 therein) and over- as well as under-estimated kernel bandwidth will result in much faster decay in MMD (see observations 1 and 3 therein). As mentioned in Theorem 1 above, the optimal EDD is proportional to the inverse of MMD, and therefore median heuristic should result in the quickest detection. We demonstrate this empirically by plotting EDD v.s. $\log \text{ARL}$, where threshold b is selected via Monte Carlo simulation to satisfy the corresponding ARL in

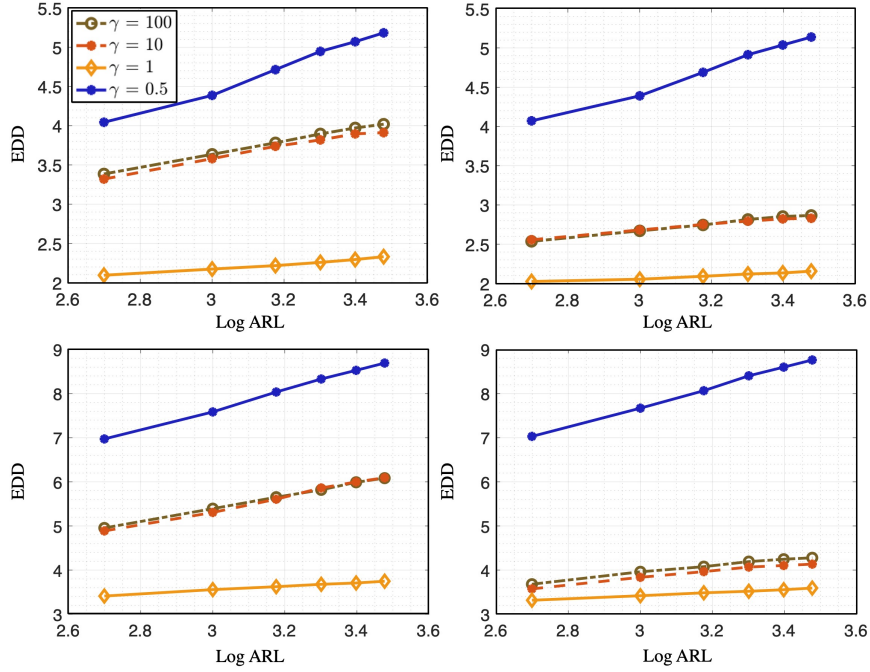


Figure 10: Comparison of EDD for different kernel bandwidths of Gaussian RBF kernel function. We consider different bandwidth choices $r = \gamma \text{med}_p$ where $\gamma \in \{0.5, 1, 10, 100\}$, where med_p is chosen via median heuristic. The change is from $\mathcal{N}(\mathbf{0}_{20}, I_{20})$ to: (a) top left: $\mathcal{N}(\mathbf{0}_{20}, 9 I_{20})$; (b) top right: $\mathcal{N}(\mathbf{1}_{20}, 9 I_{20})$; (c) bottom left: Gaussian mixture: $\mathcal{N}(\mathbf{0}_{20}, I_{20})$ w.p. 0.3; $\mathcal{N}(\mathbf{0}_{20}, 9 I_{20})$ w.p. 0.7; (d) bottom right: Gaussian mixture: $\mathcal{N}(\mathbf{0}_{20}, I_{20})$ w.p. 0.3; $\mathcal{N}(\mathbf{1}_{20}, 9 I_{20})$ w.p. 0.7.

Figure 10.

Here, we slightly abuse the notation γ : the kernel bandwidth is chosen to be $r = \gamma \text{med}_p$, where med_p denotes the median of the ℓ_2 distance matrix for pre-change samples: $\gamma < 1$ corresponds to under-estimation of kernel bandwidth whereas $\gamma > 1$ represents over-estimation. Figure 10 shows under- and over-estimation of kernel bandwidth would both lead to larger EDD and therefore median heuristic is indeed the best. Therefore, in practice, it is safe to apply the median heuristic to select kernel bandwidth.

Lastly, we study the behavior of detection statistics when choosing different N 's. Intuitively, by the Law of Large Numbers, the larger the N is, the better the performance (or convergence) of block-version MMD statistic, i.e., B -test statistic [Zaremba et al., 2013], will be. This is theoretically demonstrated in Remark 1. However, the question is, empirically speaking, how large should N be to achieve a satisfying performance? To answer this question, we plot the trajectory of the averaged detection statistic (over 50 independent runs) for our procedure in Figure 11.

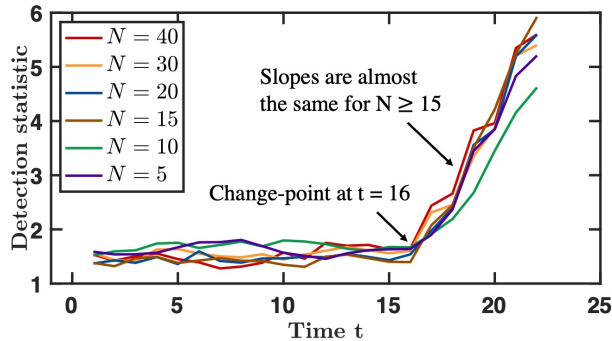


Figure 11: Comparison of mean trajectories over 50 independent trials for different pre-change blocks' numbers N . The change is from $\mathcal{N}(\mathbf{0}_{20}, I_{20})$ to Gaussian mixture with $\mathcal{N}(\mathbf{0}_{20}, I_{20})$ w.p. 0.3 and $\mathcal{N}(\mathbf{0}_{20}, 4 I_{20})$ w.p. 0.7 occurs at $t = 16$.

As we can observe in Figure 11, the slopes for $N \geq 15$ are large enough and almost the same after the change-point. We can focus on the first few steps after the change-point, since (i) we are interested in the quick detection of the change-point and (ii) the convergence of the statistic to its mean is controlled by both N and B . By taking the trade-off between the computation time and memory cost and the performance into consideration, we believe $N = 15$ suffices for our numerical simulation. However, we need to remark that, in practice, this N choice is typically determined by how many reference samples we have.

E.2 Benchmark Procedures

Before we present additional results on EDD against ARL comparison, let us briefly introduce the detection statistics of the aforementioned benchmark procedures as follows:

(a) *Scan B-statistic*: For a fixed block size $B_0 \geq 2$, the Scan B -statistic $Z_{B_0}(t)$ is defined in (3). Here, we choose $B_0 = w$, where w is the window length of our procedure.

(b) *KCUSUM statistic*: Flynn and Yoo [2019] replaced the GLR statistic in the classic CUSUM recursive update (2) with the linear-time MMD statistic [Gretton et al., 2012a] and proposed the KCUSUM procedure. The KCUSUM detection statistic has the following recursive update rule:

$$S_0^K = 0, \quad S_t^K = \begin{cases} (S_{t-1}^K + h(x_{1,t}, x_{2,t}, y_{t-1}, y_t) - \delta)^+ & \text{if } t \text{ is even,} \\ S_{t-1}^K & \text{if } t \text{ is odd,} \end{cases} \quad (48)$$

where $h(\cdot, \cdot, \cdot, \cdot)$ is defined in (6) and can be viewed as a linear-time MMD statistic with sample size $n = 2$. The hyperparameter $\delta > 0$ makes sure a negative drift and is chosen to be $\delta = 1/50$ as suggested by the original work.

(c) *Hotelling's T^2 statistic*: At time step t , for hypothetical change-point $\kappa < t$, we split the sample points into two parts: $U = (X_1, X_2, \dots, X_M, Y_1, \dots, Y_{\kappa-1})$, $V = (Y_\kappa, \dots, Y_t)$. For notational simplicity, we denote the elements in U and V by $U_1, \dots, U_{M+\kappa-1}$ and $V_1, \dots, V_{t-\kappa+1}$, respectively. We define

$$T_t^2(\kappa) = \frac{(M + \kappa - 1)(t - \kappa + 1)}{M + t} (\bar{U} - \bar{V})^\top \hat{\Sigma}^{-1} (\bar{U} - \bar{V}),$$

where $\bar{U} = \sum_{i=1}^{M+\kappa-1} U_i / (M + \kappa - 1)$, $\bar{V} = \sum_{i=1}^{t-\kappa+1} V_i / (t - \kappa + 1)$ and $\hat{\Sigma}$ is the pooled covariance matrix:

$$\hat{\Sigma} = (M + t - 2)^{-1} \left(\sum_{i=1}^{M+\kappa-1} (U_i - \bar{U})(U_i - \bar{U})^\top + \sum_{i=1}^{t-\kappa+1} (V_i - \bar{V})(V_i - \bar{V})^\top \right).$$

The Hotelling's T^2 detection statistic is defined as follows:

$$S_t^{\text{HT}^2} = \max_{1 \leq \kappa \leq t-1} T_t^2(\kappa).$$

Table 5: EDDs for given ARLs. The change is from standard Gaussian distribution $\mathcal{N}(\mathbf{0}_{20}, I_{20})$ to Gaussian mixture distribution. Non-value “–” indicates the corresponding detection procedure fails to detect the change within the first 50 time steps under the corresponding setting. Smallest EDDs are highlighted in bold fonts.

SETTING I: $\mathcal{N}(\mathbf{0}_{20}, I_{20})$ v.s. GAUSSIAN MIXTURE WITH $\mathcal{N}(\mathbf{0}_{20}, I_{20})$ w.p. 0.3; $\mathcal{N}(\mu\mathbf{1}_{20}, \sigma^2 I_{20})$ w.p. 0.7.															
ARL	$(\mu = 0.1, \sigma^2 = 0.1)$			$(\mu = 0.1, \sigma^2 = 0.3)$			$(\mu = 0.1, \sigma^2 = 1)$			$(\mu = 0.1, \sigma^2 = 4)$			$(\mu = 0.1, \sigma^2 = 9)$		
	500	1000	2000	500	1000	2000	500	1000	2000	500	1000	2000	500	1000	2000
PROPOSED	19.2	19.55	21.57	–	–	–	–	–	–	6.99	7.08	7.66	3.47	3.49	3.6
SCAN B	28.1	28.7	30.83	–	–	–	–	–	–	15.48	15.91	17.36	9.63	9.94	10.98
KCUSUM	–	–	–	–	–	–	–	–	–	–	–	–	6.03	6.89	–
HOTELLING T^2	–	–	–	–	–	–	–	–	–	–	–	–	10.04	10.46	12.17
ARL	$(\mu = 0.3, \sigma^2 = 0.1)$			$(\mu = 0.3, \sigma^2 = 0.3)$			$(\mu = 0.3, \sigma^2 = 1)$			$(\mu = 0.3, \sigma^2 = 4)$			$(\mu = 0.3, \sigma^2 = 9)$		
	500	1000	2000	500	1000	2000	500	1000	2000	500	1000	2000	500	1000	2000
PROPOSED	12.55	12.77	14.19	17.26	17.53	19.46	–	–	–	6.69	6.77	7.33	3.46	3.47	3.61
SCAN B	22.36	22.93	24.84	24.87	25.5	27.61	–	–	–	14.85	15.28	16.69	9.53	9.85	10.91
KCUSUM	–	–	–	–	–	–	–	–	–	–	–	–	6.04	6.71	8.18
HOTELLING T^2	–	–	–	–	–	–	–	–	–	17.34	17.88	–	8.88	9.28	10.68
ARL	$(\mu = 1, \sigma^2 = 0.1)$			$(\mu = 1, \sigma^2 = 0.3)$			$(\mu = 1, \sigma^2 = 1)$			$(\mu = 1, \sigma^2 = 4)$			$(\mu = 1, \sigma^2 = 9)$		
	500	1000	2000	500	1000	2000	500	1000	2000	500	1000	2000	500	1000	2000
PROPOSED	3.33	3.34	3.45	3.63	3.67	4.05	4.79	4.85	5.26	4.65	4.7	5.15	3.36	3.37	3.46
SCAN B	9.64	10.01	11.11	10.11	10.46	11.69	11.39	11.81	13.23	11.16	11.56	12.94	9.07	9.36	10.41
KCUSUM	–	–	–	–	–	–	–	–	–	–	–	–	5.16	5.85	6.73
HOTELLING T^2	9.25	9.56	10.53	9.12	9.36	10.39	8.72	8.96	9.91	7.13	7.42	8.34	5.52	5.71	6.43
ARL	$(\mu = 1.5, \sigma^2 = 0.1)$			$(\mu = 1.5, \sigma^2 = 0.3)$			$(\mu = 1.5, \sigma^2 = 1)$			$(\mu = 1.5, \sigma^2 = 4)$			$(\mu = 1.5, \sigma^2 = 9)$		
	500	1000	2000	500	1000	2000	500	1000	2000	500	1000	2000	500	1000	2000
PROPOSED	3.12	3.13	3.18	3.16	3.17	3.21	3.3	3.3	3.39	3.62	3.64	3.86	3.32	3.32	3.38
SCAN B	7.18	7.31	8.24	7.33	7.48	8.5	8.06	8.39	9.35	9.27	9.62	10.72	8.75	8.98	10.01
KCUSUM	3.99	4.05	4.08	4.1	4.18	4.28	4.95	5.3	5.86	7.05	8.37	–	4.78	5.07	5.62
HOTELLING T^2	5.74	5.86	6.59	5.72	5.87	6.51	5.63	5.8	6.34	5.11	5.24	5.77	4.37	4.49	4.98
ARL	$(\mu = 2, \sigma^2 = 0.1)$			$(\mu = 2, \sigma^2 = 0.3)$			$(\mu = 2, \sigma^2 = 1)$			$(\mu = 2, \sigma^2 = 4)$			$(\mu = 2, \sigma^2 = 9)$		
	500	1000	2000	500	1000	2000	500	1000	2000	500	1000	2000	500	1000	2000
PROPOSED	2.89	2.89	2.97	2.95	2.96	3.03	3.11	3.12	3.16	3.31	3.33	3.38	3.28	3.29	3.33
SCAN B	5.94	6.44	7.11	6.39	6.74	7.19	7.02	7.17	7.87	8.32	8.62	9.49	8.53	8.71	9.68
KCUSUM	3.98	3.98	4.01	3.98	4	4.01	4.03	4.03	4.08	4.77	5.07	5.56	4.4	4.59	4.89
HOTELLING T^2	4.31	4.38	5.17	4.34	4.44	5.08	4.37	4.45	4.92	4.14	4.24	4.6	3.72	3.82	4.16

Table 6: EDDs for given ARLs under more settings. The change is from standard Gaussian distribution $\mathcal{N}(\mathbf{0}_{20}, I_{20})$ to Laplace distribution. The best results are highlighted in bold fonts.

SETTING II: $\mathcal{N}(\mathbf{0}_{20}, I_{20})$ v.s. Laplace($\mu \mathbf{1}_{20}, b \mathbf{1}_{20}$).															
ARL	$(\mu = 0.1, b^2 = 0.1)$			$(\mu = 0.1, b^2 = 0.3)$			$(\mu = 0.1, b^2 = 1)$			$(\mu = 0.1, b^2 = 4)$			$(\mu = 0.1, b^2 = 9)$		
	500	1000	2000	500	1000	2000	500	1000	2000	500	1000	2000	500	1000	2000
PROPOSED	10.16	10.33	11.33	15.91	16.17	17.73	–	–	–	4.64	4.69	5.01	2.37	2.38	2.54
SCAN B	21.75	22.1	23.64	25.73	26.44	28.69	–	–	–	11.25	11.6	12.99	6.82	7.03	7.7
KCUSUM	–	–	–	–	–	–	–	–	–	–	–	–	3.67	4.19	5.06
HOTELLING T^2	–	–	–	–	–	–	–	–	–	–	–	–	7.03	7.35	8.47
ARL	$(\mu = 0.3, b^2 = 0.1)$			$(\mu = 0.3, b^2 = 0.3)$			$(\mu = 0.3, b^2 = 1)$			$(\mu = 0.3, b^2 = 4)$			$(\mu = 0.3, b^2 = 9)$		
	500	1000	2000	500	1000	2000	500	1000	2000	500	1000	2000	500	1000	2000
PROPOSED	6.43	6.51	7.23	8.92	9.04	9.97	17.9	18.26	20.22	4.4	4.46	4.76	2.34	2.36	2.5
SCAN B	15.88	16.21	17.92	18.01	18.56	20.48	23.82	24.42	26.67	10.53	10.9	12.22	6.72	6.96	7.59
KCUSUM	–	–	–	–	–	–	–	–	–	–	–	–	3.62	4.12	4.83
HOTELLING T^2	24.95	25.4	27.12	24.11	24.56	26.1	20.89	21.38	23.08	11.83	12.31	13.99	6.12	6.43	7.31
ARL	$(\mu = 0.5, b^2 = 0.1)$			$(\mu = 0.5, b^2 = 0.3)$			$(\mu = 0.5, b^2 = 1)$			$(\mu = 0.5, b^2 = 4)$			$(\mu = 0.5, b^2 = 9)$		
	500	1000	2000	500	1000	2000	500	1000	2000	500	1000	2000	500	1000	2000
PROPOSED	4.15	4.18	4.6	5.08	5.17	5.65	7.51	7.61	8.32	4.05	4.07	4.35	2.3	2.31	2.45
SCAN B	12.07	12.56	13.49	13.06	13.41	14.49	15.1	15.51	16.97	9.58	9.98	11.19	6.62	6.86	7.48
KCUSUM	–	–	–	–	–	–	–	–	–	–	–	–	3.45	3.97	4.65
HOTELLING T^2	14.66	14.83	15.45	14.32	14.52	15.28	13.04	13.32	14.35	8.42	8.75	9.94	5.28	5.52	6.27
ARL	$(\mu = 0.7, b^2 = 0.1)$			$(\mu = 0.7, b^2 = 0.3)$			$(\mu = 0.7, b^2 = 1)$			$(\mu = 0.7, b^2 = 4)$			$(\mu = 0.7, b^2 = 9)$		
	500	1000	2000	500	1000	2000	500	1000	2000	500	1000	2000	500	1000	2000
PROPOSED	3.81	3.86	3.99	3.9	3.93	4.03	4.58	4.63	4.96	3.61	3.64	3.89	2.25	2.25	2.38
SCAN B	8.94	9.23	10.45	9.5	9.87	11.02	10.97	11.36	12.71	8.6	8.94	10.11	6.53	6.72	7.35
KCUSUM	–	–	–	–	–	–	–	–	–	–	–	–	3.28	3.73	4.39
HOTELLING T^2	9.69	9.98	10.94	9.33	9.66	10.78	8.51	8.82	9.93	6.41	6.62	7.49	4.6	4.79	5.4
ARL	$(\mu = 1.5, b^2 = 0.1)$			$(\mu = 1.5, b^2 = 0.3)$			$(\mu = 1.5, b^2 = 1)$			$(\mu = 1.5, b^2 = 4)$			$(\mu = 1.5, b^2 = 9)$		
	500	1000	2000	500	1000	2000	500	1000	2000	500	1000	2000	500	1000	2000
PROPOSED	2	2	2	2	2	2	2.03	2.03	2.06	2.25	2.27	2.43	2.03	2.04	2.07
SCAN B	5	5	5.77	5	5.03	5.95	5.47	5.68	6.28	6.26	6.44	7.1	6.05	6.15	7
KCUSUM	2.01	2.03	2.05	2.07	2.11	2.18	2.54	2.72	2.94	3.52	3.99	4.81	2.48	2.75	3.06
HOTELLING T^2	4.01	4.05	4.93	4.06	4.12	4.76	4.06	4.14	4.51	3.66	3.74	4.11	3.12	3.21	3.57

Table 7: EDDs for given ARLs under more settings. The change is from standard Gaussian distribution $\mathcal{N}(\mathbf{0}_{20}, I_{20})$ to Uniform distribution. The best results are highlighted in bold fonts.

SETTING III: $\mathcal{N}(\mathbf{0}_{20}, I_{20})$ v.s. $U[(a-b)\mathbf{1}_{20}, (a+b)\mathbf{1}_{20}]$.															
ARL	$(a = 0.1, b^2 = 0.1)$			$(a = 0.1, b^2 = 0.3)$			$(a = 0.1, b^2 = 1)$			$(a = 0.1, b^2 = 4)$			$(a = 0.1, b^2 = 9)$		
	500	1000	2000	500	1000	2000	500	1000	2000	500	1000	2000	500	1000	2000
PROPOSED	6	6	6.93	5.26	5.39	5.99	4	4	4	2.06	2.07	2.18	2	2	2
SCAN B	16	16.02	18	13.96	14.22	15.23	10.36	10.74	11.66	6.17	6.41	7.08	5.07	5.21	5.98
KCUSUM	—	—	—	—	—	—	—	—	—	3.67	4.2	5.08	2.18	2.23	2.33
HOTELLING T^2	29.1	29.46	30.77	20.28	20.61	22.21	12.3	12.65	13.41	5.19	5.31	5.95	3.95	4	4.26
ARL	$(a = 0.3, b^2 = 0.1)$			$(a = 0.3, b^2 = 0.3)$			$(a = 0.3, b^2 = 1)$			$(a = 0.3, b^2 = 4)$			$(a = 0.3, b^2 = 9)$		
	500	1000	2000	500	1000	2000	500	1000	2000	500	1000	2000	500	1000	2000
PROPOSED	4	4	4.51	4	4	4	2.92	2.99	3.52	2	2	2	2	2	2
SCAN B	12.63	13	13.97	10.66	10.98	11.91	7.54	7.98	9.06	5.48	5.79	6.25	5	5.01	5.61
KCUSUM	—	—	—	—	—	—	—	—	—	2.4	2.55	2.83	2.05	2.07	2.1
HOTELLING T^2	15.77	15.99	16.89	13.03	13.17	14.03	7.55	7.92	9.17	4.8	4.89	5.05	3.5	3.64	3.98
ARL	$(a = 0.7, b^2 = 0.1)$			$(a = 0.7, b^2 = 0.3)$			$(a = 0.7, b^2 = 1)$			$(a = 0.7, b^2 = 4)$			$(a = 0.7, b^2 = 9)$		
	500	1000	2000	500	1000	2000	500	1000	2000	500	1000	2000	500	1000	2000
PROPOSED	2.01	2.02	2.95	2	2	2	2	2	2	2	2	2	2	2	2
SCAN B	7	7	8.1	6.28	6.96	7.03	5.67	5.98	6.27	5	5	5.21	4.97	5	5
KCUSUM	6.71	—	—	3.88	4.77	6.2	2.37	2.55	2.84	2.01	2.02	2.03	2	2	2
HOTELLING T^2	7	7	8.07	6	6.06	7	5	5	5.4	3.92	3.97	4.04	3	3.01	3.16
ARL	$(a = 1.5, b^2 = 0.1)$			$(a = 1.5, b^2 = 0.3)$			$(a = 1.5, b^2 = 1)$			$(a = 1.5, b^2 = 4)$			$(a = 1.5, b^2 = 9)$		
	500	1000	2000	500	1000	2000	500	1000	2000	500	1000	2000	500	1000	2000
PROPOSED	2	2	2	2	2	2	2	2	2	2	2	2	2	2	2
SCAN B	5	5	5	5	5	5	4.12	4.99	5	4	4.09	5	4.05	4.69	5
KCUSUM	2	2	2	2	2	2	2	2	2	2	2	2	2	2	2
HOTELLING T^2	4	4	4	4	4	4	3	3.02	3.97	2.96	2.99	3	2.05	2.1	2.6
ARL	$(a = 2, b^2 = 0.1)$			$(a = 2, b^2 = 0.3)$			$(a = 2, b^2 = 1)$			$(a = 2, b^2 = 4)$			$(a = 2, b^2 = 9)$		
	500	1000	2000	500	1000	2000	500	1000	2000	500	1000	2000	500	1000	2000
PROPOSED	2	2	2	2	2	2	2	2	2	2	2	2	2	2	2
SCAN B	4	4	5	4	4	5	4	4	5	4	4	5	4.01	4.45	5
KCUSUM	2	2	2	2	2	2	2	2	2	2	2	2	2	2	2
HOTELLING T^2	3	3	3	3	3	3	3	3	3	2.01	2.04	2.74	2	2	2.01

E.3 EDD against ARL Comparison under More Settings

To further demonstrate the good performance of our procedure, we additionally consider more settings for (i) change from Gaussian to Gaussian mixture as well as change from Gaussian distribution to (ii) Laplace and (iii) uniform distributions. The results are reported in Tables 5, 6 and 7, respectively. From these tables, we can observe that our proposed online kernel CUSUM achieves the quickest detection among all benchmarks, even under the settings where the changes are too small for parametric procedures to detect. In addition to the aforementioned observations, we can see Hotelling’s T^2 procedure performs pretty well when the mean shift is significant but fails easily otherwise. Under those small mean shift circumstances, kernel methods can easily achieve better performance than Hotelling’s T^2 procedure; see the first two rows in the table for evidence. This observation agrees with our intuition since Hotelling’s T^2 procedure is a parametric method that is designed to detect the mean shift.

E.4 Real Example: HASC Dataset

The HASC dataset is publicly available and contains measurements of human activities for 6 human subjects (indexed by 101, 102, 103, 105, 106, 107) and 6 types of activities (jog, walk, skip, stay, stair down, stair up). For those 6 human subjects, there are 10, 15, 10, 15, 15, 15 repeats taken, respectively; for each single repeat, the sequence length is around 2000. Those repeats may correspond to activity under different conditions, e.g., floor types (asphalt or carpet), weather (for outdoor activities, including fine, cloudy, rain, snow) and so on; however, we treat them as different repeats of the same for simplicity. We need to mention that there are only 3 repeats taken for subject 107 staring up and thus this scenario is left out in our experiment.

Here, the goal of online change-point detection is: for a chosen human subject, given history activity data (e.g., walking) and assuming we receive sequential data of this subject from the accelerometers, we want to detect the activity change (e.g., change to staying) as soon as possible. As an illustrative example, we choose human subject 101 and take walk as the pre-change activity; we visualize the 3-dimensional raw data of one trial in Figure 12. As one can see, there is a clear cyclic pattern; although we assume the data points are i.i.d., we take into account this particular structure when constructing the pre-change blocks: we first partition this history data based on its peaks into 15 segments; then, we choose the minimum segment length as the window length (i.e., $w = 114$); finally, we use the first 14 segments with equal length as the pre-change blocks (i.e., $N = 14$). In addition, the kernel bandwidth

is chosen by using the median heuristic on this whole history data sequence, which gives us $r = 0.865$.

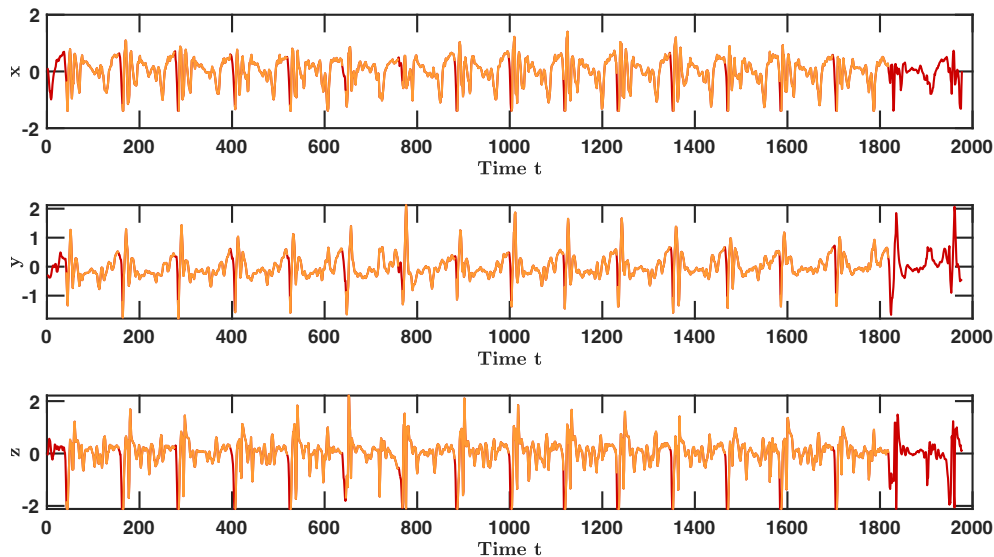


Figure 12: Visualization of the history data for subject 101’s walking activity. The raw data is in red; we partition this whole sequence into 15 segments with equal length 114 (highlighted in orange).

For completeness, we carry out the aforementioned experiment for the rest 5 human subjects and report the EDD over successfully detected changes and miss in Table 8, where the detection threshold is again chosen as the 80% quantile of the maximum detection statistics under H_0 (i.e., the post-change activity is still walking). In this table, we highlight the best procedure for each human subject based on the miss (i.e., fewer misses means a better procedure).

From Table 8, we can make the following additional observations: (i) The KUSUM-type procedures based on non-parametric kernel MMD statistics do perform pretty well. (ii) The detection can be difficult for certain human subjects and certain repeats (since those repeats are carried out under different settings); in contrast, it is easier to detect the change for subjects 105 as well as 106, and we can see our procedure outperforms other benchmarks in the sense that it is the most robust one (i.e., it have the smallest number of misses), and oftentimes it has the smallest EDD. These findings further demonstrate the usefulness of our proposed online kernel CUSUM procedure in practice.

Table 8: EDD and miss of human activity change detection in HASC dataset. The pre-change activity is walking. The best results are highlighted in bold fonts.

SUBJECT 102 (IN TOTAL 15 REPEATS).										
ACTIVITY	JOG		SKIP		STAY		STAIR DOWN		STAIR UP	
	EDD	Miss	EDD	Miss	EDD	Miss	EDD	Miss	EDD	Miss
PROPOSED	320	13	–	15	–	15	–	15	–	15
SCAN <i>B</i>	320	13	–	15	–	15	–	15	–	15
KCUSUM	886	13	1034	12	–	15	1707	13	–	15
HOTELLING T^2	–	15	–	15	–	15	–	15	–	15

SUBJECT 103 (IN TOTAL 10 REPEATS).										
ACTIVITY	JOG		SKIP		STAY		STAIR DOWN		STAIR UP	
	EDD	Miss	EDD	Miss	EDD	Miss	EDD	Miss	EDD	Miss
PROPOSED	483.5	6	391.5	8	855.25	6	–	10	–	10
SCAN <i>B</i>	637	1	95.67	7	861	6	–	10	–	10
KCUSUM	348.6	0	333.2	0	–	10	1266	9	80	9
HOTELLING T^2	320.67	7	104	9	875.25	6	–	10	–	10

SUBJECT 105 (IN TOTAL 15 REPEATS).										
ACTIVITY	JOG		SKIP		STAY		STAIR DOWN		STAIR UP	
	EDD	Miss	EDD	Miss	EDD	Miss	EDD	Miss	EDD	Miss
PROPOSED	260.93	0	49.6	0	3426.5	13	206.89	6	490.1	5
SCAN <i>B</i>	108	3	87.13	0	1591	13	775.43	8	884.29	8
KCUSUM	395.67	3	362.53	0	–	15	–	15	98	14
HOTELLING T^2	905	13	178.25	3	3328.5	13	521.2	10	931	8

SUBJECT 106 (IN TOTAL 15 REPEATS).										
ACTIVITY	JOG		SKIP		STAY		STAIR DOWN		STAIR UP	
	EDD	Miss	EDD	Miss	EDD	Miss	EDD	Miss	EDD	Miss
PROPOSED	121.1	5	124.4	0	19.5	13	584.5	11	430.25	7
SCAN <i>B</i>	368.14	8	162.4	0	19.5	13	334	12	137.4	5
KCUSUM	563.5	7	722.29	1	–	15	884	13	–	15
HOTELLING T^2	176.11	6	66.4	0	23	13	629	12	333.25	7

SUBJECT 107 (IN TOTAL 15 REPEATS).										
ACTIVITY	JOG		SKIP		STAY		STAIR DOWN		STAIR UP	
	EDD	Miss	EDD	Miss	EDD	Miss	EDD	Miss	EDD	Miss
PROPOSED	–	15	641.4	10	–	15	–	15	–	–
SCAN <i>B</i>	–	15	–	15	–	15	–	15	–	–
KCUSUM	814.31	2	813.78	6	–	15	1151.2	10	–	–
HOTELLING T^2	1917	13	1038	14	–	15	–	15	–	–